Environmental controls on the growth, photosynthetic and calcification rates of a Southern Hemisphere strain of the coccolithophore *Emiliania huxleyi*

Yuanyuan Feng,[1,2]* Michael Y. Roleda,[2,3] Evelyn Armstrong,[4] Philip W. Boyd,[5] Catriona L. Hurd[2,5]
[1]College of Marine and Environmental Sciences, Tianjin University of Science and Technology, Tianjin, China
[2]Department of Botany, University of Otago, Dunedin, New Zealand
[3]Norwegian Institute of Bioeconomy Research, Bodø, Norway
[4]Department of Chemistry, NIWA/University of Otago Research Centre for Oceanography, University of Otago, Dunedin, New Zealand
[5]Institute for Marine and Antarctic Studies, University of Tasmania, Hobart, Tasmania, Australia

Abstract

We conducted a series of diagnostic fitness response experiments on the coccolithophore, *Emiliania huxleyi*, isolated from the Subtropical Convergence east of New Zealand. Dose response curves (i.e., physiological rate vs. environmental driver) were constructed for growth, photosynthetic, and calcification rates of *E. huxleyi* relative to each of five environmental drivers (nitrate concentration, phosphate concentration, irradiance, temperature, and pCO$_2$). The relative importance of each environmental driver on *E. huxleyi* rate processes was then ranked using a semi-quantitative approach by comparing the percentage change caused by each environmental driver on the measured physiological metrics under the projected conditions for the year 2100, relative to those for the present day, in the Subtropical Convergence. The results reveal that the projected future decrease in nitrate concentration (33%) played the most important role in controlling the growth, photosynthetic and calcification rates of *E. huxleyi*, whereas raising pCO$_2$ to 75 Pa (750 ppm) decreased the calcification : photosynthesis ratios to the greatest degree. These findings reveal that other environmental drivers may be equally or more influential than CO$_2$ in regulating the physiological responses of *E. huxleyi*, and provide new diagnostic information to better understand how this ecologically important species will respond to the projected future changes to multiple environmental drivers.

Coccolithophores are a group of calcium carbonate (CaCO$_3$) producing phytoplankton, which have a global distribution (Moore et al. 2012) from the high latitudes of the Northern Hemisphere to the "great calcite belt" of the Southern Ocean (Balch et al. 2011). They play important roles in the global carbon cycle through both organic carbon fixation by photosynthesis and CaCO$_3$ production by calcification (Milliman 1993; Westbroek et al. 1993; Rost and Riebesell 2004); the latter may further change the marine carbonate system by releasing CO$_2$ and decreasing seawater alkalinity (Riebesell et al. 2009). Over the last decade, research has suggested that coccolithophores may be susceptible to projected changes in oceanic conditions driven by climate change (Langer et al. 2006; Beaufort et al. 2011;

Raven and Crawfurd 2012), especially ocean acidification (OA), the change in the seawater carbonate system caused by increased anthropogenic CO$_2$ emission into the atmosphere (Caldeira and Wickett 2003). The potential responses of coccolithophores to future changes in the marine environment will consequently alter their role in the oceanic carbon cycle, a topic that has received widespread attention (Raven et al. 2005; Smith et al. 2012).

Emiliania huxleyi is the most abundant coccolithophore species, forming large blooms that are readily observed using satellite imagery of the oceans (Holligan et al. 1983, 1993; Westbroek et al. 1993; Honisch et al. 2012). Due to its global distribution, *E. huxleyi* populations have high genetic variability (Iglesias-Rodriguez et al. 2006) and five morphotypes (A, B, B/C, C, and R; Young and Westbroek 1991). There are a growing number of studies suggesting differential responses across different *E. huxleyi* strains/morphotypes to the changes in seawater carbonate chemistry (summarized in Table 1). Some studies indicate decreased *E. huxleyi*

*Correspondence: yfeng@tust.edu.cn

Table 1. Trends in the physiological responses of E. huxleyi to changes in pCO_2 (reported as the pCO_2 range of conditions) summarized from published studies. Data are presented on the location of the isolate, incubation conditions (nitrate, phosphate, irradiance, and temperature), and seawater carbonate chemistry manipulation methods (CO_2 man.), particulate organic carbon productivity (POC prod.), particulate inorganic carbon productivity (PIC prod.), cellular particulate organic carbon (POC) content and the cellular PIC : POC ratio. "↑" represents increase, "↓" represents decrease and "nc" represents no significant change to altered environmental conditions. POC prod./PIC prod. with asterisks (*) indicate productivity which were calculated based on growth rate and cellular POC and PIC contents instead of from direct measurements.

Northern Hemisphere E. huxleyi strains

E. huxleyi strain	Isolation location	Morph.	Nitrate μM	Phosphate μM	Irradiance μmol photons m⁻² s⁻¹	Temp. °C	pCO₂ range ppm	μ	POC μ prod.	PIC prod.	Cellular POC	Cellular PIC	Cellular PIC : POC	CO₂ man.†	Reference
AC481	North Sea; 49°30′N 2°30′E		32	1	150	13	180,379,740	→			nc	nc	nc	1	De Bodt et al. (2010)
AC481	49°30′N 2°30′E		32	1	150	18	180,379,740	nc			nc	nc	nc	1	De Bodt et al. (2010)
Bergen	North Sea 60°30′N 5°30′E		88	3.6	140	16	380–1000	→			←	→	→	3; long-term	Müller et al. (2010)
CCMP371	Sargasso Sea, 50m depth; 32°N 62°W	B/C	882	36.2	50	20	380, 750	nc	←		nc	nc	nc	1	Feng et al.(2008)
CCMP371		B/C	882	36.2	400	20	380, 750	←	←		↑↓	→	→	1	Feng et al.(2008)
CCMP371		B/C	882	36.2	50	24	380, 750	nc	←		nc	nc	nc	1	Feng et al.(2008)
CCMP371		B/C	882	36.2	400	24	380, 750	←	nc		nc	→	→	1	Feng et al.(2008)
Ch 24-90	North Sea	B/C	250	25	300	15	50–780	nc	←	←			nc	1	Buitenhuis et al. (1999)
RCC1256	North Atlantic, off Iceland; 63°24′N 20°20′W	A	100	6.25	400	17	200–900	→			←	←	nc	3	Langer et al. (2009)
RCC1256		A	100	6	170	15	300–1200	→	nc*	↓*	nc	←	→	3	Hoppe et al. (2011)
RCC1256		A	100	6	170	15	200–850	→	↓*	↓*	nc	←	→	1	Hoppe et al. (2011)
		A	441	5	150	15	209–1255	↑↓						2	Hermoso et al. (2016)
Natural population	North Sea 60°18′N 5°12′W		15.3	0.5	127–836 95% of I_0‡	10-13	190–713		←	←	→		→	1	Engel et al. (2005)
Natural Population	North Atlantic; 57°35′N		5	0.31	30% of I_0‡	12	390,690	nc	nc	nc			nc	1	Feng et al. (2009)
Natural Population	15°19′W		5	0.31	100–300 30% of I_0‡	16	390, 690	nc	nc	→		→	→	1	Feng et al. (2009)
PMLB92/11A	North Sea 60°16′N 5°14′W	A	100	6.25	150	15	100–900	nc			↑	→	→	3	Riebesell et al. (2000b)
PMLB92/11A		A	100	6.25	150	15	100–900		↑*	↓*		→	→	3	Zondervan et al. (2001)
PMLB92/11A		A	100	6.25	15, 30, 80	15	100–900	nc			↑	→	→	3	Zondervan et al. (2002)
PMLB92/11A		A	64	4	150	10	380–750	→	↑*	nc*		→	→	2	Sett et al. (2014)
PMLB92/11A		A	64	4	150	15	380–750	nc	↑*	↓*		→	→	2	Sett et al. (2014)
PMLB92/11A		A	64	4	150	20	380–750	←	↑*	↑*		→	→	2	Sett et al. (2014)

TABLE 1. Continued

E. huxleyi strain	Isolation location	Morph.	Nitrate μM	Phosphate μM	Irradiance μmol photons $m^{-2} s^{-1}$	Temp. °C	pCO_2 rangeppm	μ	POC prod.	PIC prod.	Cellular POC	Cellular PIC	Cellular PIC:POC	CO_2 man.†	Reference
RCC1238	North Pacific, off Japan; 34°01′N 139°50′E	A	100	6.25	400	20	200–900	↑			→	nc	nc	3	Langer et al. (2009)
TW1	W Mediterranean; 39°30′N 1°30′E		14–15.5	5	170	17	404, 718			→	→	→	nc	1	Sciandra et al. (2003)
Southern Hemisphere E. huxleyi strains															
AC 472 diploid	South Pacific, Western New Zealand	R	160	10	160	19	400, 760	↑			nc	↑	↑	1	Fiorini et al. (2011)
AC 472 haploid	Zealand	R	160	10	160	19	400, 760	↑			→		→	1	Fiorini et al. (2011)
NZEH	South Pacific, off	R	100	6.25	150	20	380, 750	↑			↑	↑	→	3	Shi et al. (2009)
NZEH	New Zealand	R	100	6	170	15	200–1200	nc	nc*	↓*	nc	→	→	3	Hoppe et al. (2011)
NZEH		R	100	6	170	15	200–1100	nc	nc*	↓*	nc	→	→	1	Hoppe et al. (2011)
NZEH		R	150	3	120	19	250–1314				↑	↑	nc	2	Rouco et al. (2013)
NZEH		R	3	3	120	19	250–1314				↑	nc	↑	2	Rouco et al. (2013)
NZEH		R	150	0.2	120	19	250–1314				↑↓	↑↓	↑↓	2	Rouco et al. (2013)
NZEH		R	100	6.25	150	19	280–750	→			↑	↑	nc	1	Iglesias-Rodriguez et al. (2008)
NZEH		R	100	6.25	150	20	380, 750	nc			nc	nc	nc	1	Shi et al. (2009)
RCC1212	South Atlantic, off South Africa; 34°28′S 17°18′E	B	100	6.25	400	20	200–1100	→			nc	→	→	3	Langer et al. (2009)
RCC1216	Tasman Sea; 42°18′S 169°50′E	R	100	6.25	400	17	200–1200	nc	nc*		nc	→	→	3	Langer et al. (2009)
RCC1216		R	100	6.25	50	15	400–1200	nc	↑*	↓*	↑	→	→	1	Rokitta and Rost (2012)
RCC1216		R	100	6.25	300	15	400–1200	nc	nc*	nc*	↑	nc	nc	1	Rokitta and Rost (2012)
EHTB 11.15	Trumpeter Bay, Tasmania; 43°S, 147°E	A over-calcified	88	3.6	110	14	375–1652	nc	↑↔*	nc			→	2	Müller et al. (2015)
EHBH 13.28	Bicheno, Tasmania; 42°S, 148°E	A over-calcified	88	3.6	110	14	349–1513	nc	↑↔*	nc		→	→	2	Müller et al. (2015)
EHSO 5.14	Southern Ocean; 50°S, 149°E	A	88	3.6	110	14	300–1683	→	nc*	↓*		→	→	2	Müller et al. (2015)
EHSO 5.30		A	88	3.6	110	14	296–1747	→	nc*	↓*		→	→	2	Müller et al. (2015)

TABLE 1. Continued

E. huxleyi strain	Isolation location	Morph.	Nitrate μM	Phosphate μM	Irradiance μmol photons m⁻² s⁻¹	Temp. °C	pCO2 range ppm	μ	POC prod.	PIC prod.	Cellular POC	Cellular PIC	Cellular PIC : POC	CO2 man.†	Reference
	Southern Ocean; 50°S, 149°E														
EHSO 5.11	Southern Ocean; 50°S, 149°E	B/C	88	3.6	110	14	259–1255	↓	↑↓*	↑↓*			↑↓	2	Müller et al. (2015)
EHSO 8.15	Southern Ocean; 54°S, 146°E	B/C	88	3.6	110	14	244–1306	↓	↑↓*	↑↓*			↑↓	2	Müller et al. (2015)
NIWA1108	Chatham Rise, South Pacific, off New Zealand 43°S 176°E	A	96	6	140	14	79–1080	↑↓	↑→	↓	nc	nc	→	1	This study

Morph., Morphotype; temp., temperature; prod., production.
†CO_2 manipulation methods: 1-DIC manipulation by bubbling with air-CO_2 mixtures; 2-DIC manipulation by adding $NaHCO_3$/Na_2CO_3 and HCl; and 3-TA manipulation without changing DIC concentration by only adding NaOH or HCl.
‡I_0 represents the sea surface irradiance.

calcification rates under rising pCO_2 (Riebesell et al. 2000; Zondervan et al. 2001; Feng et al. 2008); however, contradictory results of increased calcification due to rising pCO_2 have also been reported (Iglesias-Rodriguez et al. 2008; Shi et al. 2009), suggesting strain-specific responses (Langer et al. 2009; Langer 2011). This diversity of responses by E. huxleyi demonstrates the complexity in understanding the regulatory mechanisms of this ecologically important calcifier to changes in seawater carbonate chemistry (see summaries of Findlay et al. 2011; Hoppe et al. 2011; Raven and Crawfurd 2012).

In addition to seawater carbonate chemistry, other environmental factors will change simultaneously due to future global climate change, such as temperature (Bopp et al. 2001) and mixed layer depth in some areas (Sarmiento et al. 2004). Changes to the mixed layer depth will alter the upper ocean integrated irradiances, and increased density stratification will diminish the vertical nutrient supply to phytoplankton (Boyd and Doney 2002). Each of these environmental factors may regulate different cellular processes of E. huxleyi in various ways. For example, light (Nimer and Merrett 1993), nutrient concentration (Paasche and Brubak 1994; Langer and Benner 2009) and temperature (Paasche 1968) may all influence the calcification rate of E. huxleyi. In the present study, these environmental factors are referred to as "drivers," which is defined by Boyd and Hutchins (2012) as "an environmental change that results in a quantifiable biological response, ranging from stress to enhancement." Moreover, these environmental drivers not only affect E. huxleyi physiology individually, but also have interactive effects and modulate the responses of E. huxleyi to OA (reviewed by Paasche 2002; Zondervan 2007; Raven and Crawfurd 2012). For example, nitrogen source (Lefebvre et al. 2012), light intensity (Rokitta and Rost 2012) and temperature (Sett et al. 2014) could all modulate the CO_2 effects on calcification of E. huxleyi (strains CCMP 371, RCC 1216, and PML 92/11, respectively) either by altering resource allocation or energy availability.

Most of the previous laboratory and field studies on the responses of E. huxleyi to environmental change have focused on Northern Hemisphere isolates and less information is available for Southern Hemisphere strains (Stojkovic et al. 2013). However, coccolithophore blooms are equally influential in the southern hemisphere based on ocean color satellite imagery (Moore et al. 2012), especially with the widespread observation of the "Great Calcite Belt" in the Southern Ocean (Balch et al. 2011). Genetic differences between Southern and Northern Hemisphere E. huxleyi strains have been reported, based on micro-satellite analysis (Iglesias-Rodriguez et al. 2006). As such, it can be speculated that the physiological responses of the Southern Hemisphere strains to global climate change would be different to their Northern Hemisphere counterparts.

Despite the available extensive studies on the physiology of coccolithophores, especially on Northern Hemisphere strains (Paasche 2002; Zondervan 2007), to date there has been no systematic examination of how projected marine environmental changes, especially to multiple environmental drivers, will affect coccolithophore physiology of either the Northern or the Southern Hemisphere strains. This is due to most previous studies focusing mainly on the effects of a single environmental driver, and there are only a few attempts examining the interactions between two or three drivers (e.g., Feng et al. 2008; Sett et al. 2014). Boyd et al. (2010) provided the first attempt to rank the importance of the environmental drivers (such as temperature, irradiance, nitrogen, phosphorus, and iron) on controlling coccolithophores based on evidence in published literature. Boyd et al. suggested that temperature may play the most important role in regulating coccolithophore physiology. Such ranking provides a helpful diagnostic tool to explore how changes in these environmental drivers, both individually and interactively, will affect phytoplankton groups (Boyd et al. 2010). In the present study, we used climate model projections for the Subtropical Convergence, a circumpolar boundary between subantarctic and subtropical waters east of New Zealand, to project changes in five environmental drivers which are known to affect *E. huxleyi* physiology: nitrate concentration, phosphate concentration, irradiance, temperature, and $p\mathrm{CO_2}$. Here, in order to better predict how *E. huxleyi* will respond to future changes of multiple environmental drivers, we conducted a series of manipulation experiments on an *E. huxleyi* strain isolated from this region to assess the relative importance of each environmental driver on the physiological rate processes (growth, photosynthetic and calcification rates) of *E. huxleyi*.

Materials and methods

Experimental setup

The coccolithophore, *E. huxleyi* (strain NIWA1108), was isolated from the Chatham Rise, the location of the circumpolar Subtropical Convergence east of New Zealand by Dr. H. Chang (NIWA) in November 2008. The Chatham Rise region is characterized by non-limiting concentrations of dissolved iron that are supplied from subtropical waters east of New Zealand (Boyd et al. 1999). The stock culture was maintained in the laboratory at 14°C and at 140 μmol photons m^{-2} s^{-1}, under a 12 h/12 h light/dark cycle. The media used for maintaining the stock culture and the manipulation experiments were made with aged coastal seawater from Otago Harbour (45.9°S, 170.5°E) (salinity 34.5; phosphate 0.3–0.4 μM, nitrate 3–6 μM, silicate 4–6 μM), filtered through a 0.2 μm pore size filtration cartridge (Whatman^{TM}). For the stock culture, the medium was supplemented with nutrients to give a final phosphate concentration of 6 μM and nitrate of 96 μM, without silicate addition. Trace metals and

vitamins were added to f/20 level [10 times dilution of f/2 trace metal and vitamin recipe (Guillard and Ryther 1962)]. The trace metal and vitamin concentrations were kept at these levels in all of the manipulation experiments.

The design of each manipulation experiment was analogous to a reaction norm (i.e., fitness vs. environment; Woltereck 1909; Gabriel and Lynch 1992) and was based on defining the response of a range of physiological rates, such as calcification, to changes in the environment. To begin the manipulation experiments, *E. huxleyi* cells in exponential growth phase were transferred into 500-mL polycarbonate bottles with screw caps and subjected to a series of semi-continuous incubation experiments under different nutrient, irradiance, temperature, and $p\mathrm{CO_2}$ conditions. Only one driver was manipulated at a time in each experiment, with the levels of the other drivers remaining the same as the stock culture growing conditions. Initial cell abundances were diluted to $\sim 10^4$ cells mL^{-1} in all bottles and in vivo chlorophyll *a* (Chl *a*) fluorescence was monitored daily as an indicator of Chl *a* biomass and cell growth (Gilbert et al. 2000). After 2–3 d of acclimation under the experimental conditions, daily dilution was started using freshly made seawater medium added into each bottle to adjust the biomass to that of the previous day. Triplicate bottles for each set of conditions were incubated. All of the experiments were carried out in a walk-in growth chamber, with overhead metal halide lamps (full spectrum) as the light source, and a light/dark cycle of 12 h/12 h. Irradiance levels for all the manipulation experiments were measured by submerging a quantum PAR sensor inside the incubation bottles.

The phosphate manipulation experiment was performed using five treatments: 0.4 (seawater background concentration) μM, 2 μM, 6 μM, 10 μM, and 20 μM. Six treatments were examined in the nitrate manipulation: 3.7 (background) μM, 6 μM, 12 μM, 48 μM, 96 μM, and 200 μM. For the irradiance manipulation, six treatments were examined: 14 μmol photons m^{-2} s^{-1}, 40 μmol photons m^{-2} s^{-1}, 80 μmol photons m^{-2} s^{-1}, 190 μmol photons m^{-2} s^{-1}, 350 μmol photons m^{-2} s^{-1}, and 650 μmol photons m^{-2} s^{-1}. These irradiance levels were obtained by wrapping bottles with different layers of neutral density screen. Temperature (14°C) during the irradiance manipulation was controlled by submerging the bottles in a tank connected to a chiller (HC150A, Hailea, China) via a water pump.

Six treatments were examined in the temperature manipulation: 4°C, 7°C, 11°C, 15°C, 20°C, and 25°C. The cultures at 4°C were acclimated to the low temperature gradually by growing stock cultures at 7°C for 3 d and then transferring them to 4°C for the experiment. In all cases, temperature in each tank was monitored continuously, with variation less than $\pm$ 0.5°C.

For the $\mathrm{CO_2}$ manipulation, six $p\mathrm{CO_2}$ treatments (8 Pa, 15 Pa, 39 Pa, 58 Pa, 74 Pa, and 109 Pa; equivalent to 79 ppm, 150 ppm, 382 ppm, 568 ppm, 733 ppm, and 1080 ppm)

were examined. Seawater media were pre-adjusted to the desired condition by bubbling with nitrogen gas (for 8 Pa, 15 Pa, and 39 Pa) or 10% CO_2 in air (for 58 Pa, 74 Pa, and 109 Pa) before the daily dilution of the cultures. The caps of the incubation bottles were designed with a pH sampling port and gas in- and out-flow ports. CO_2 concentrations were maintained in the bottles by gentle bubbling of certified commercial CO_2 and air gas mixtures, at the corresponding concentrations, through Tygon^{TM} tubing connected with the gas in-flow ports. The pH ports were connected to an automated spectrophotometric pH measurement system (Mcgraw et al. 2010) to measure the pH of all treatments before and after their daily dilution. The monitored pH values were relatively constant ($\pm$ 0.015) during the incubation period and the difference in the seawater carbonate chemistry between the culture medium and within the incubation bottles was small (Supporting Information Table S1).

The final sampling was not performed until after the growth rate, which was monitored daily, became relatively constant (i.e., daily variations < 10%) for more than seven generations (Feng et al. 2008). This enabled acclimation of the cultures to the experimental conditions for ~20 d. Subsamples from each bottle were collected for cell counts, Chl *a* biomass, elemental components [Particulate Organic Carbon (POC), Particulate Inorganic Carbon (PIC), Particulate Organic nitrogen (PON), and Particulate Organic Phosphorus (POP)], calcification and photosynthetic rates, morphological analysis of the coccoliths using Scanning Electron Microscopy (SEM), and for seawater carbonate chemistry analysis.

Sample analyses

Cell counts and Chl a

Samples for cell counts were preserved by adding 6 μL modified Lugol's solution (dissolving 10 g KI and 5 g iodine crystals in 20 mL Milli-Q water, then adding 50 mL of 5% anhydrous sodium acetate solution; (Utermöhl 1958) to 1 mL of sample, and then kept in the dark at 4°C. Samples were counted with a nanoplankton counting chamber (PhycoTech, U.S.A.) using a Zeiss microscope (Axiostar plus, Germany) at ×200 magnification. In vivo Chl *a* fluorescence was measured daily within 2 h of the start of the light period for consistency in measuring the daily growth rate using fluorometry. For in vitro Chl *a* concentration at the end of the experiment, samples were obtained and analyzed following procedures in (Welschmeyer 1994). Growth rate (μ) was calculated using in vivo Chl *a* fluorescence daily as: $\mu = \ln[N(T_2)/N(T_1)]/(T_2 - T_1)$, in which $N(T_1)$ and $N(T_2)$ are the in vivo Chl *a* fluorescence values at T_1 and T_2.

Photosynthetic and calcification rates

The ^{14}C incubation technique (Paasche 1964; Paasche et al. 1996) was used to determine photosynthetic and calcification rates. Within the first 3 h of the light phase on the final sampling day, two 50 mL subsamples from each triplicate bottle were spiked with 2 μCi NaH^{14}CO$_3$. One

subsample was incubated in the light and the other in the dark for 4 h. Then two sets of 25 mL aliquots from each subsample were filtered onto Whatman GF/F filters. The filters for photosynthetic rate determination were fumed with saturated HCl before adding scintillation cocktail fluid (Hisafe3, Perkin-Elmer, U.S.A.). Photosynthetic rate and calcification rate was calculated as described in Paasche et al. (1996). The elemental composition of *E. huxleyi* is described and discussed in Feng (2015) and Feng et al. (unpubl.).

Seawater carbonate chemistry

Samples (250 mL) for alkalinity analysis were preserved with 200 μL of 5% HgCl$_2$ solution in glass bottles (Schott AG, Germany) with screw caps. Alkalinity was measured using potentiometric titration following the method of Dickson et al. (2007). The accuracy of the method, as determined by analysis of Certified Reference Material (Andrew Dickson, Scripps Institution of Oceanography) was $\pm$ 2 μmol kg^{-1}. The measurements were conducted using a Fluke high precision voltmeter, and the final calculation was carried out using custom-written software (K. Currie pers. comm.).

For DIC measurements, 20 mL borosilicate vials were filled with samples avoiding the formation of air bubbles, and fixed by adding 20 μL 5% HgCl$_2$ solution. The samples were capped tightly and stored at 4°C in the dark until analysis. DIC concentrations were analyzed with an automated infra-red inorganic carbon analyzer (AIRICA, MARIANDA, Germany) connected with a LI-COR 820, and corrected to the Dickson seawater standards (Dickson et al. 2007). The estimated accuracy of the analysis was $\pm$5 μmol kg^{-1}. Total scale pH values (pH$_T$) were measured by a colorimetric method with thymol blue as an indicator dye using the automated seawater pH measurement system (Mcgraw et al. 2010). The seawater carbonate chemistry was calculated using the program CO2sys version 1.05 (E. Lewis and D. W. R. Wallace), using the constants in Mehrbach et al. (1973), re-fitted by Dickson and Millero (1987).

Coccolith morphology

Samples for scanning electron microscopy were rinsed with Milli-Q water and filtered onto 0.6 μm porosity polycarbonate filters under 5–10 mm Hg of vacuum. The filters were then air-dried, mounted on stubs and coated with gold before examination by scanning electron microscope (JEOL Ltd, Tokyo, Japan) at the Otago Centre of Electron Microscopy. More than 20 individual cells and 100 coccoliths from each treatment were then randomly selected from the field of view and photographed at magnification of ×6000–×9000 (Henderiks et al. 2012).

Data analyses

Fitting of reaction norms

The reaction norms were fitted using the examined growth, photosynthetic and calcification rates on the final sampling day (acclimatized steady-state growth phase) and the environmental conditions at which the cultures were

Percentage change = (V1-V2)/V1×100%
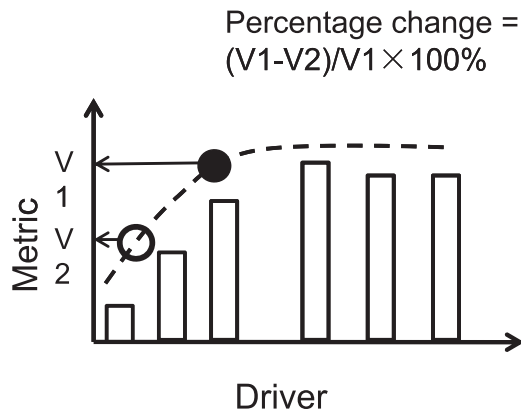
Fig. 1. Conceptual cartoon of the ranking scheme used to assess the relative importance of each of the environmental drivers on the physiological metrics of *E. huxleyi* in the present study. *Dashed line indicates the fitted reaction norm. The filled symbol represents the present day condition, and the open symbol indicates the projected condition for the year 2100. V1 and V2 are the values of the physiological metric (such as growth rate) on the response curve for present day and projected (year 2100) conditions, respectively. Ranking was performed based on the absolute values of the calculated percentage changes caused by each driver.

incubated. The dose-response curves of growth, photosynthetic, and calcification rate vs. nitrate and phosphate concentration and the growth rate vs. pCO_2 were fitted to the Michaelis–Menten function (Michaelis and Menten 1913). The growth and calcification rate vs. irradiance curves and the growth rate of steady growth phase/photosynthetic rate/ calcification rate vs. pCO_2 curves were all fitted using the Monod function with an inhibition term after Litchman (2000) and Megard et al. (1984).

The growth, photosynthetic, and calcification rate vs. temperature curves along with the calcification : photosynthesis (Cal : Photo hereafter) ratio vs. temperature were fitted using the thermal tolerance function described in Thomas et al. (2012). A photosynthesis vs. irradiance function with a photo-inhibition term (Webb et al. 1974; Sakshaug et al. 1997) was used to fit the photosynthetic rate vs. irradiance response curves.

The Cal : Photo ratio vs. nitrate concentration and phosphate concentration curves were fitted using a modified Monod function. The Cal : Photo ratio vs. irradiance curve

was fitted using a one phase decay model; while the Cal : Photo ratio vs. pCO_2 curve was fitted with a linear regression model.

All of the curve-fitting was performed using a least square fit with Prism software (version 5.0; GraphPad Prism Software, San Diego, CA, USA) and the triplicate data for each treatment. The equations for the fittings and fitted constants and the parameters of goodness of fit generated from each fitting are presented in Supporting Information Table S2.

Statistical analyses

The effects of each driver on the physiological rates of *E. huxleyi* were determined with one-way analysis of variance. Differences between treatments were considered significant at $p < 0.05$. Post-hoc comparisons were conducted using the Student–Neuman–Keuls (SNK) test to determine any pairwise differences.

Ranking the importance of the environmental drivers

A semi-quantitative approach was used to rank the relative importance of individual drivers on each physiological process. First, the specific physiological metric (such as growth or calcification rate) at the (mean) present-day condition (e.g., filled symbol in Fig. 1) and the projected condition for 2100 (Table 2; Boyd and Law 2011; Rickard et al. unpubl.), were derived from the fitted dose-response curve for each driver. The magnitude and direction of change in each physiological metric was calculated as the percentage change of the projected future (2100) condition relative to that for the present day (Table 2). The ranking was then performed by comparing the values of the percentage changes of each physiological parameter caused by each driver. The driver that caused the largest change was ranked as the most influential controlling factor, and vice versa. This approach was used as an initial assessment to examine the importance of the changes of the five drivers on the physiology of *E. huxleyi* by 2100.

Although the models used for data-fitting were carefully selected based on prior publications, there are limitations in the model fitting and hence the propagation of errors, causing inevitable mismatches between the model predictions and the measured values (Barry and Elith 2006). Therefore, it is important to recognize that there are instances where the model prediction indicates an increase or decline in a certain physiological metric but the results of the ANOVA (within a

Table 2. The selected values for each of the environmental drivers in the control, present day, and future Chatham Rise conditions. "Control" represents the stock culture growth conditions, "Present day" represents the present day average values for surface waters in the Chatham Rise region, and "Future" represents the model projections for the upper ocean in Chatham Rise region for 2100.

Driver Condition	Nitrate (μM)	Phosphate (μM)	Irradiance (μmol photons m^{-2} s^{-1})	Temperature (°C)	pCO_2 (Pa)
Control	96	6	140	14	39
Present day	10	1	140	14	39
Future	6.7	0.67	175	16	75
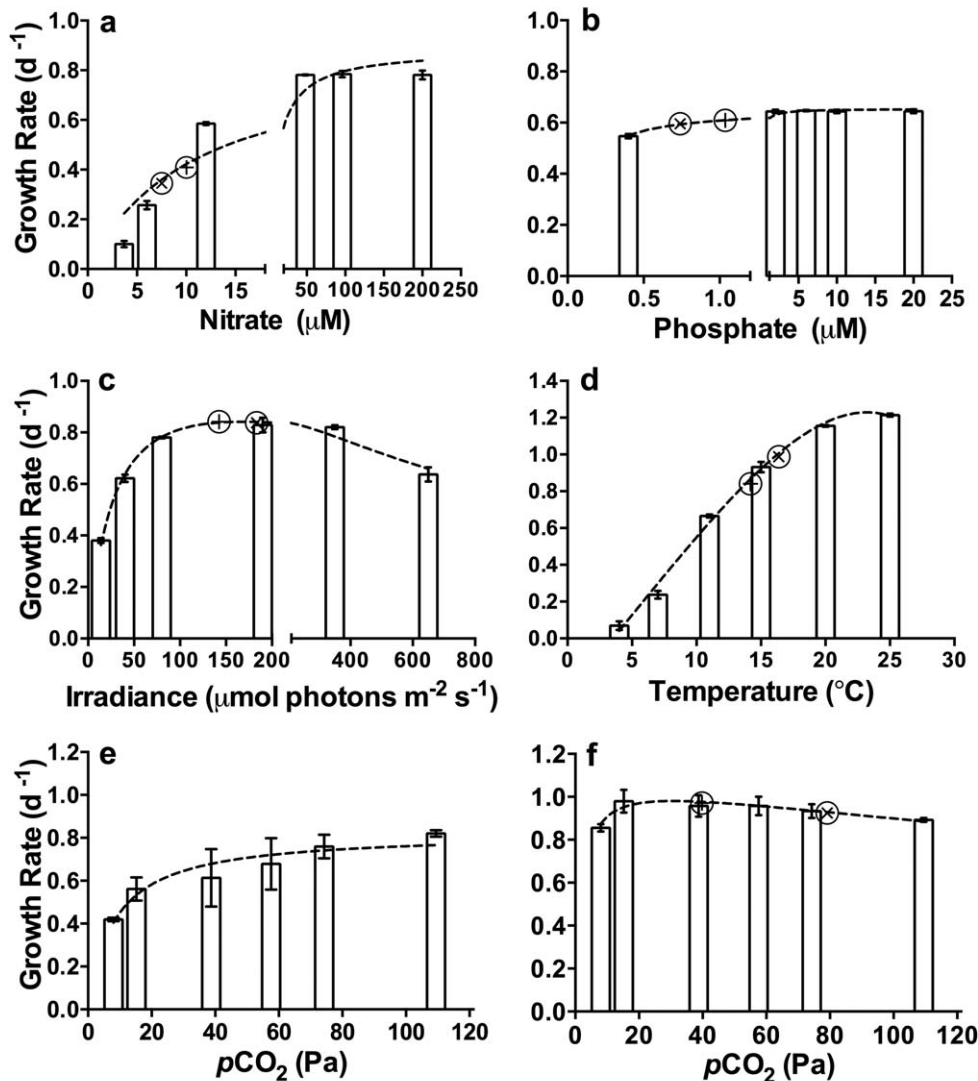
Fig. 2. Changes in *E. huxleyi* growth rate on the final sampling day (except for e) in response to individual environmental drivers: (**a**) growth rate vs. nitrate concentration; (**b**) growth rate vs. phosphate concentration; (**c**) growth rate vs. irradiance; (**d**) growth rate vs. temperature; (**e**) average growth rate of day 4–8 vs. pCO_2; and (**f**) growth rate of the steady growth phase vs. pCO_2.

similar range of values) indicates that the difference is not significant. For example, the fitted dose-response curve indicated a decreasing trend of growth rate with rising pCO_2 from 39 Pa to 74 Pa, while one-way ANOVA results suggest no significant difference between the two CO_2 treatments. Therefore, some of the ranking results need to be treated with caution, considering the uncertainties due to the errors around the mean values of the measurements

Results

Environmental controls on growth rate

The growth rate of *E. huxleyi* increased with nitrate until 50 μM, where it plateaued (Fig. 2a). At the lowest concentration examined (3.7 μM), growth rate (0.10 ± 0.01 d^{-1}) was

$\sim$90% lower than the (fitted) maximum growth rate μ_{max} (0.88 ± 0.04 d^{-1}; Fig. 2a; Supporting Information Table S2). In contrast to nitrate, the growth rate of *E. huxleyi* remained relatively constant across all phosphate concentrations (Fig. 2b). Growth increased by 18% between 0.4 μM and 2 μM, from 0.55 ± 0.01 d^{-1} to 0.64 ± 0.01 d^{-1}, with no change at higher concentrations. The half saturation constant of phosphate for growth (K_m) was 0.11 ± 0.01 μM, and the ratio of K_m between nitrate and phosphate was $\sim$100.

Increasing irradiance promoted the growth of *E. huxleyi*, with a maximum growth rate at $\sim$100 μmol photons m^{-2} s^{-1} (Fig. 2c). Photo-inhibition was observed at the highest irradiance examined (650 μmol photons m^{-2} s^{-1}), with the growth rate 30% lower than μ_{max} of 0.91 ± 0.05 d^{-1} ($p = 0.001$). Growth rate increased significantly with
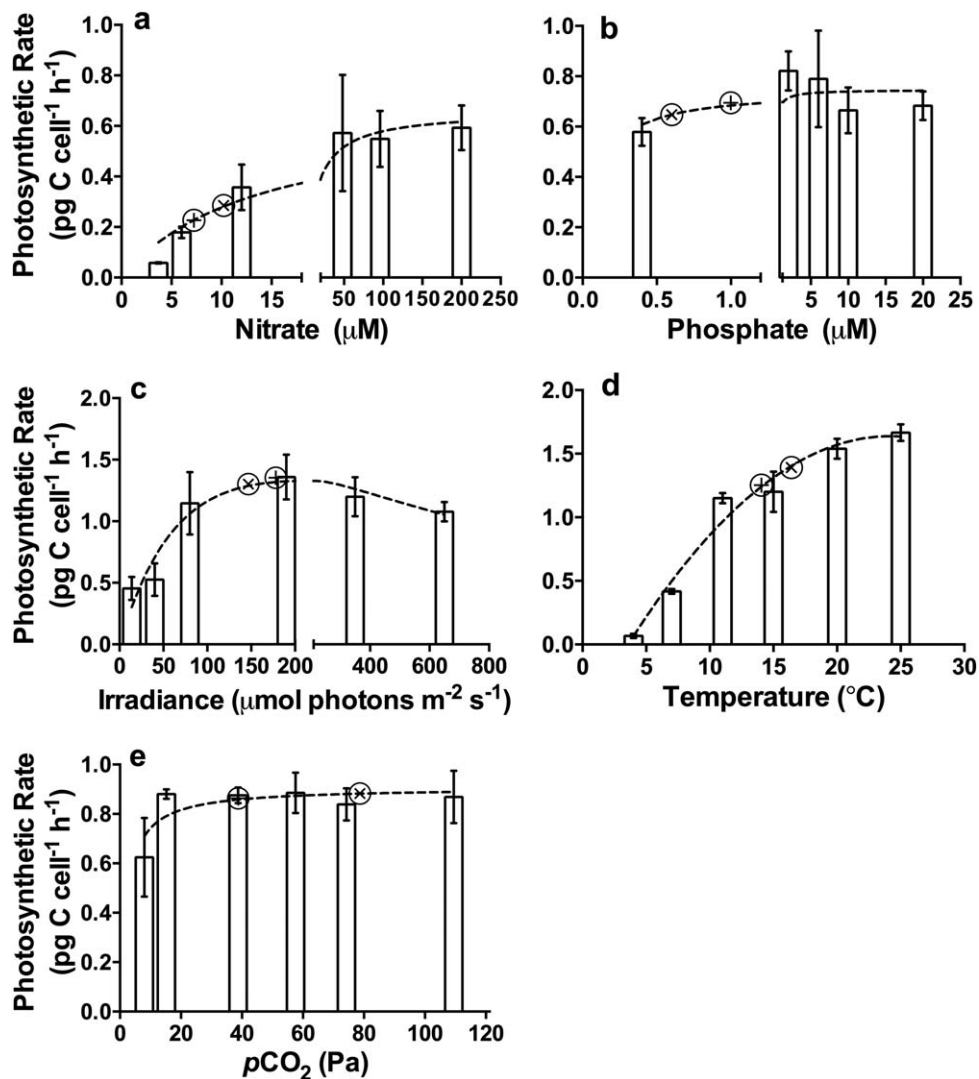
Fig. 3. Alteration of *E. huxleyi* photosynthetic rate on the final sampling day in response to individual drivers: (**a**) photosynthetic rate vs. nitrate concentration; (**b**) photosynthetic rate vs. phosphate concentration; (**c**) photosynthetic rate vs. irradiance; (**d**) photosynthetic rate vs. temperature; and (**e**) photosynthetic rate vs. pCO_2.

warming, from 0.07 ± 0.02 d^{-1} at 3°C to 1.21 ± 0.01 d^{-1} at 25°C ($p < 0.001$; Fig. 2d). The fitted growth rate vs. temperature response curve resulted in an optimal temperature of 23°C with highest growth of ~ 1.23 d^{-1}, $\sim 20\%$ higher than that at 14°C (i.e., the stock culture condition).

A trend of acclimation by *E. huxleyi* to altered pCO_2 was observed during the incubation. At the beginning, growth rate increased with rising pCO_2; the average rate from day 4 to 8 was lowest (0.42 ± 0.01 d^{-1}) at 8 Pa and highest (0.82 ± 0.02 d^{-1}) at 109 Pa (Fig. 2e). However, growth continued to increase in all treatments, until the acclimatized steady growth phase was reached on day 9. On the final sampling day, there was no significant difference among the growth rates in the four pCO_2 treatments between 15 Pa and 74 Pa, whereas the growth rates at 8 Pa (0.85 ± 0.02 d^{-1}) and

109 Pa (0.89 ± 0.01 d^{-1}) were both slightly lower than the other four treatments ($p = 0.03$, $p = 0.04$ respectively, Fig. 2f).

Response of photosynthetic and calcification rates to different drivers

Nutrients

Nitrate concentration greatly affected the photosynthetic rate of *E. huxleyi* within the tested range (Fig. 3a). The fitted half saturation constant K_m was 13.71 ± 4.74 μM, close to the value for growth rate (Supporting Information Table S2). Photosynthetic rate increased 10-fold ($p < 0.001$) from 0.06 ± 0.00 pg C cell^{-1} h^{-1} at 3.7 μM nitrate to P_{max} of 0.66 ± 0.06 pg C cell^{-1} h^{-1} at ~ 50 μM nitrate and plateaued at that point, similar to the growth vs. nitrate response. In the case of phosphate (Fig. 3b), the photosynthetic rate of
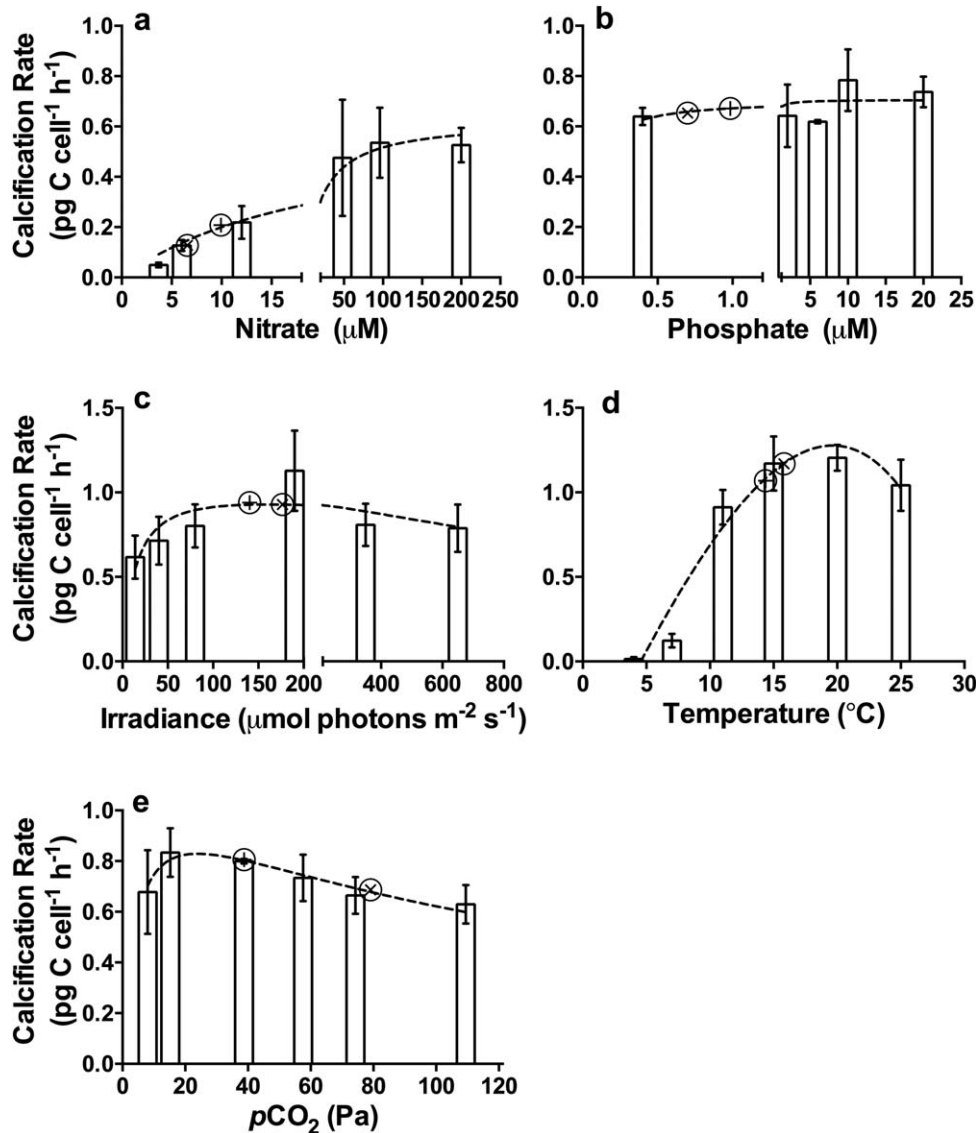
Fig. 4. Changes in *E. huxleyi* calcification rate on the final sampling day in response to individual drivers: (**a**) calcification rate vs. nitrate concentration; (**b**) calcification rate vs. phosphate concentration; (**c**) calcification rate vs. irradiance; (**d**) calcification rate vs. temperature; and (**e**) calcification rate vs. pCO_2.

0.58 ± 0.06 pg C cell^{-1} h^{-1} at the lowest concentration (0.4 μM) was 26% lower than that at 2 μM ($p = 0.01$). However, no further significant change in this rate was observed across other treatments (2 μM, 6 μM, 10 μM, and 20 μM P). The ratio of K_m (see Supporting Information Table S2) for photosynthetic rate between nitrate and phosphate was $\sim$114, higher than that for growth rate ($\sim$100).

The response of *E. huxleyi* calcification rate across a range of nitrate concentrations was similar to that of photosynthesis (Fig. 4a). The fitted K_m for nitrate was 21.40 ± 8.31 μM for calcification, higher than for photosynthesis (13.71 ± 4.74 μM; Supporting Information Table S2). Calcification increased at lower nitrate concentrations until reaching a

maximum at $\sim$50 μM nitrate. The ratio of calcification rate to photosynthetic rate (Fig. 5a) decreased slightly with nitrate concentration between 3.7 μM and 12 μM, with the lowest ratio at 12 μM. The ratio increased at higher nitrate concentrations, and there was no significant difference across the three highest nitrate levels tested (48 μM, 96 μM, and 200 μM; $p > 0.05$).

Calcification was relatively constant across all phosphate treatments (Fig. 4b). However, there was a 30% decrease ($p = 0.03$) in the Cal : Photo ratio when phosphate increased from 0.4 μM (1.12 ± 0.16) to 2 μM (0.78 ± 0.08). The ratio further increased from 2 μM to 10 μM phosphate (Fig. 5b). However, there was no significant difference across the four
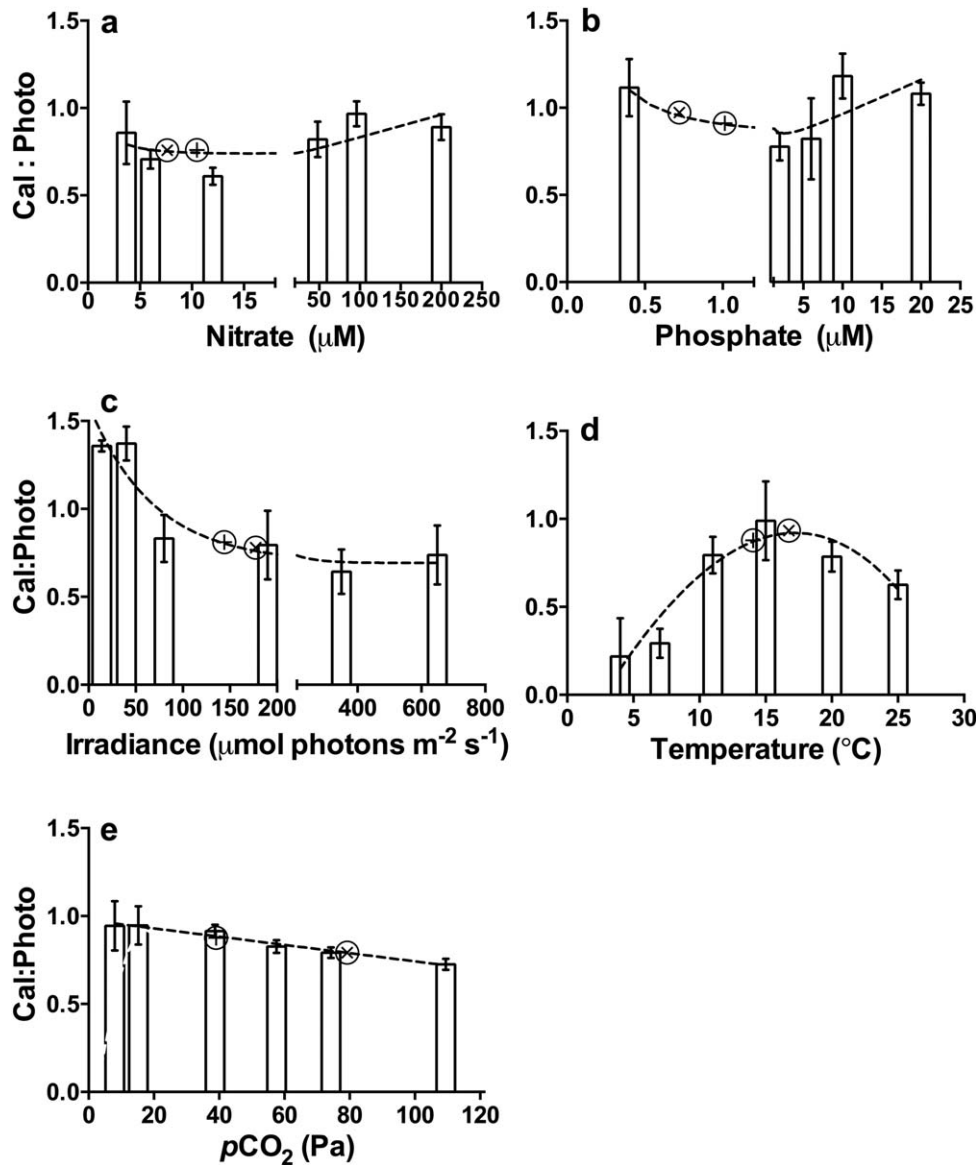
Fig. 5. Changes in *E. huxleyi* calcification: photosynthesis ratio on the final sampling day in response to individual drivers: (**a**) calcification: photosynthesis ratio vs. nitrate concentration; (**b**) calcification: photosynthesis ratio vs. phosphate concentration; (**c**) calcification: photosynthesis ratio vs. irradiance; (**d**) calcification: photosynthesis ratio vs. temperature; and (**e**) calcification: photosynthesis ratio vs. pCO_2. **For Figs. 2-5: The dashed lines represent the fitted dose-response curves. "X" denote the fitted values for present-day conditions in the Chatham Rise area, and "+" represent the fitted values for predicted future conditions (2100) in this region. Error bars represent standard deviation ($n = 3$).

phosphate treatments of 0.4 μM, 6 μM, 10 μM, and 20 μM. The lowest (fitted) Cal : Photo ratio was 0.73.

Irradiance

The photosynthetic response to irradiance (Fig. 3c) was also similar to that for growth rate. The calculated I_k value (saturation irradiance for photosynthesis) was $\sim$65 μmol m^{-2} s^{-1}. Compared to P_{max} (1.57 $\pm$ 0.24 pg C cell^{-1} h^{-1} at 190 μmol m^{-2} s^{-1}), there was a 52% decrease in photosynthetic rate (1.03 $\pm$ 0.01 pg C cell^{-1} h^{-1}) at 650 μmol m^{-2} s^{-1} ($p = 0.04$), indicating photo-inhibition. Calcification rate was highest at 190 μmol photons m^{-2} s^{-1} (1.13 $\pm$ 0.24 pg C

cell^{-1} h^{-1}), 82% higher ($p = 0.03$) than that at 14 μmol photons m^{-2} s^{-1}. Calcification then decreased at 350 μmol photons m^{-2} s^{-1} and 650 μmol photons m^{-2} s^{-1} (Fig. 4c). The Cal : Photo ratio was significantly higher (> 1.0) at 14 μmol photons m^{-2} s^{-1} and 40 μmol photons m^{-2} s^{-1} compared to the other four treatments ($p < 0.05$, Fig. 5c). The ratio declined $\sim$40% from 1.37 $\pm$ 0.10 pg C cell^{-1} h^{-1} at 40 μmol photons m^{-2} s^{-1} to 0.83 $\pm$ 0.13 pg C cell^{-1} h^{-1} at 80 μmol photons m^{-2} s^{-1} and then was relatively steady at higher irradiances with no significant difference across the four treatments.

Temperature

Warming significantly promoted the photosynthetic rate of *E. huxleyi* at the temperatures examined (Fig. 3d). Photosynthetic rate increased significantly by more than fivefold from 4°C (0.06 ± 0.02 pg C cell^{-1} h^{-1}) to 7°C (0.42 ± 0.02 pg C cell^{-1} h^{-1}; $p < 0.001$), and continued increasing to 1.66 ± 0.06 pg C cell^{-1} h^{-1} at 25°C ($p < 0.001$). The fitted response curve of photosynthetic rate vs. temperature indicated an optimal temperature for photosynthesis at ∼24°C with a calculated P_{max} of 1.64 pg C cell^{-1} h^{-1}. Calcification rate also responded significantly to temperature (Fig. 4d). As for the trends in growth and photosynthetic rate, calcification increased significantly with warming, especially between 3°C and 15°C. The fitted optimal temperature for calcification was ∼20°C, lower than those for both photosynthesis and growth. The Cal : Photo ratio was significantly lower at 4°C and 7°C (values below 0.3) compared to the other four treatments (Fig. 5d). SEM observations showed severe malformation of coccoliths (Fig. 6a,b) at 4°C and 7°C, where > 95% of the examined coccoliths were with incomplete distal shield elements. At 4°C, open central areas of the distal shields were also observed. At other temperature treatments, there was no significant coccolith malformation (see Fig. 6c for an example at 15°C); the coccoliths had robust distal shield and curved central area elements and thus the *E. huxleyi* strain was identified as morphotype A (Young et al. 2003). The Cal : Photo ratio increased with temperature and reached a maximum of 0.92 at an optimal temperature ∼17°C (Fig. 5d). The calcification to photosynthesis ratio decreased at 20°C and 25°C, with a 37% decrease at 25°C compared to the ratio at 15°C ($p = 0.04$).

CO$_2$

Changes in pCO$_2$ level did not affect the *E. huxleyi* photosynthetic rate significantly (Fig. 3e). Although the average rate was slightly lower at 8 Pa, the difference across all the pCO$_2$ treatments was not statistically significant ($p > 0.05$). There was a non-significant decrease in *E. huxleyi* calcification rate with rising pCO$_2$ at ≥ 8 Pa (Fig. 4e). In contrast, the Cal : Photo ratio decreased significantly with rising pCO$_2$, especially in the four higher pCO$_2$ treatments ($p < 0.05$; Fig. 5e). The ratio reduced by 23% from 0.94 ± 0.14 at 8 Pa to 0.72 ± 0.03 at 109 Pa linearly.

Ranking of the importance of environmental controls on *E. huxleyi* physiology

Based on the calculations of percentage changes in physiological process rates, projected for future conditions at the Subtropical Convergence relative to those in the present day conditions, nitrate played the most important role in regulating growth, photosynthetic, and calcification rate, while CO$_2$ was the most important factor affecting the Cal : Photo ratio of *E. huxleyi* (Table 3). The 33% decrease in nitrate concentration from the present day level of 10–6.7 μM resulted in the highest percentage change (20% decrease) in growth
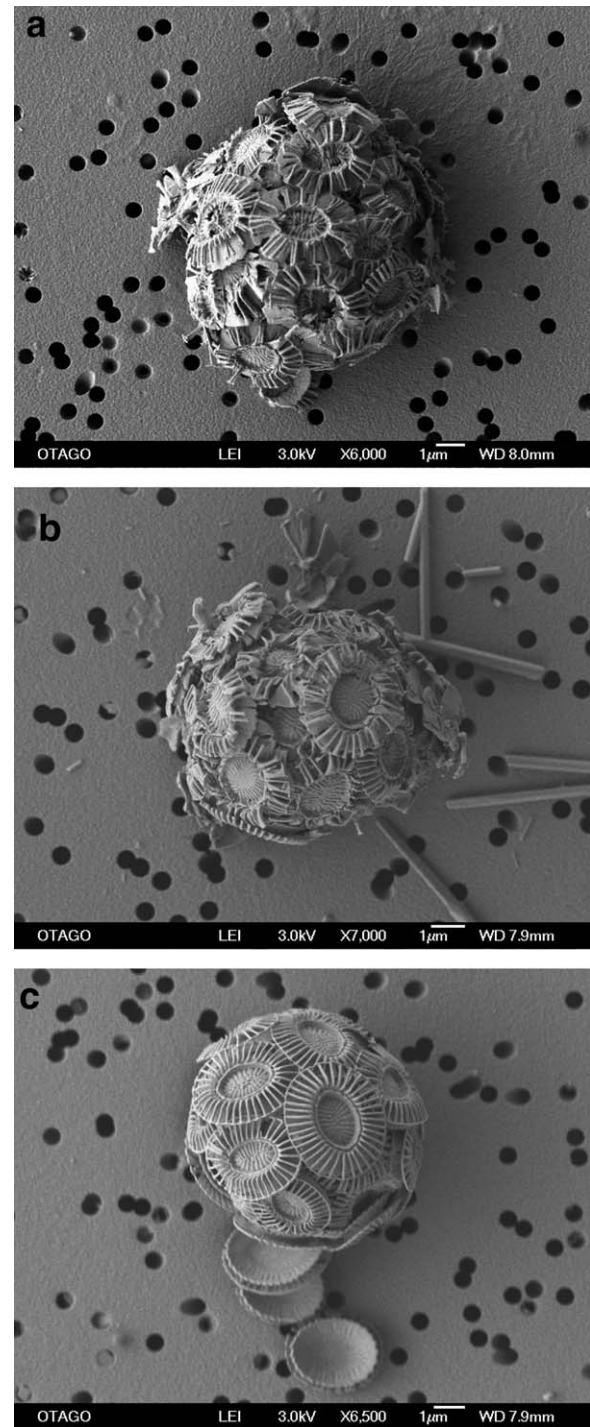
Fig. 6. Scanning electron microscopic images of *E. huxleyi* grown at different temperatures during the temperature manipulation experiment. Substantially malformed coccoliths were observed at (**a**) 4°C and (**b**) 7°C; and (**c**) normal coccoliths at 15°C.

rate among all drivers. Photosynthetic rate decreased by 22% and calcification rate declined by 25%, with a 33% decrease in nitrate concentration. For the Cal : Photo ratio, rising pCO$_2$ from 39 Pa to 74 Pa resulted in a 10% decrease.

Table 3. Comparison of growth, photosynthetic, and calcification rates, and calcification: photosynthesis ratios between projected (year 2100) and present day Chatham Rise upper ocean conditions. Rankings of the influence of each environmental driver on the physiological rate processes are expressed as follows: (1) most influential to (5) least influential. "+" represents a rate increase and "−" represents a rate decrease under future conditions relative to the present day.

		Fitted values*		Future vs. present day comparisons		
Physiological process	Environmental driver	Present day	Future	Change (%)†	Effects(+/−)	Ranking
Growth rate (d^{-1})	Nitrate	0.422	0.336	20.5	−	**1‡**
	Temperature	0.854	0.984	15.2	+	**2**
	CO_2	0.978	0.933	4.6	−	3
	Phosphate	0.608	0.588	3.3	−	**4**
	Irradiance	0.838	0.841	0.4	+	**5**
Photosynthetic rate	Nitrate	0.278	0.216	22.2	−	**1**
(pg C cell^{-1} h^{-1})	Temperature	1.237	1.379	11.5	+	2
	Phosphate	0.684	0.657	3.9	−	3 (n.s.)
	Irradiance	1.276	1.317	3.2	+	4
	CO_2	0.858	0.881	2.8	+	5
Calcification rate	Nitrate	0.200	0.150	25.1	−	**1**
(pg C cell^{-1} h^{-1})	CO_2	0.804	0.688	14.4	−	2 (n.s.)
	Temperature	1.057	1.181	11.8	+	3
	Phosphate	0.672	0.656	2.3	−	4 (n.s.)
	Irradiance	0.927	0.928	0.1	+	5
Calcification: Photosynthesis	CO_2	0.887	0.799	9.9	−	**1**
	Phosphate	0.906	0.967	6.8	+	**2**
	Irradiance	0.810	0.764	5.8	−	3
	Temperature	0.870	0.913	4.9	+	4
	Nitrate	0.744	0.756	1.6	+	**5**

*The fitted values for "control," "present day," and "future" were extracted from the dose-response curves (Figs. 2-5) based on the stock-culture growing conditions, average present day conditions (Chatham Rise), and the projected future conditions (2100) (Table 2), respectively.
†Percentage changes were calculated as the differences caused by each environmental driver on these physiological processes under the future conditions relative to that under present day conditions.
‡Numbers in bold indicate statistically significant difference between the present day and future conditions (nitrate treatments: 6.0 μM and 12.0 μM; phosphate treatments: 0.4 μM and 2 μM; irradiance treatments: 80 μmol photons m^{-2} s^{-1} and 190 μmol photons m^{-2} s^{-1}; temperature treatments: 11°C, 15°C, and 20°C) based on the one-way ANOVA. "n.s." indicates non-significant difference (one-way ANOVA) among all the treatments used for the fitting.

Discussion

Effects of nitrate and phosphate concentrations on *E. huxleyi* physiology

Nitrate concentration ranked as the most important driver controlling *E. huxleyi* growth, photosynthetic, and calcification rates in our study. Nitrate may be important in *E. huxleyi* physiology for three reasons. First, since nitrogen is an essential element for nucleic acid and protein synthesis, nitrate limitation might decrease the production of some proteins which are important transporters in photosynthesis and calcification (Raven and Crawfurd 2012). This may explain why in the present study the Cal : Photo ratio was not greatly affected by nitrate limitation since the two rates decreased to a similar degree with lower nitrate concentrations. Moreover, for calcification, these proteins may include DIC transporters in carbon concentrating mechanism (CCM) (Quigg et al. 2011) as well as Ca^{2+}, H^+, and HCO_3^-

transporters (Mackinder et al. 2011). Second, nitrogen is the element for synthesizing the organic matrix materials of coccoliths and so nitrate limitation may affect coccolith formation of *E. huxleyi* (Paasche 1964; Nimer and Merrett 1993; Sciandra et al. 2003).

Nitrate concentration played a more important role than phosphate in regulating the growth rate of *E. huxleyi*. Here, the ratio of the half saturation constants between these two inorganic nutrients was ∼100, approximately six times the Redfield ratio of 16 (Redfield et al. 1963). Previous studies also suggest that *E. huxleyi* is, in general, a poor competitor for nitrate (Riegman et al. 1992). However, it has a much higher affinity for phosphate than other phytoplankton species (Riegman et al. 2000), with the ability to utilize organic phosphorus forms with the cell-surface bound enzyme, alkaline phosphatase (Riegman et al. 1992; Falkowski et al. 2004; Arrigo 2005). The above discrepancy in *E. huxleyi* phosphate

and nitrate affinities in our study also explains the lack of a physiological response to increased phosphate compared to nitrate concentration. In addition, the biomineralization pathway in *E. huxleyi* is mainly based on acidic polysaccharides (APSs), which bind calcium ions and regulate the crystallization of calcium carbonate, and are able to bind to a positively charged protein at the end of the crystallization process (Westbroek et al. 1984; Marsh 1994). This mechanism is different from other biomineralization pathways, such as silicification in diatoms. The latter is mainly energized by oxidative phosphorylation (Blank et al. 1986) and protein based (Frigeri et al. 2006). Therefore, *E. huxleyi* is likely to be much more competitive, compared to other phytoplankton groups, under phosphate-limiting conditions, in both the Northern and Southern Hemisphere. This assertion provides a compelling explanation for other research that observed blooms of *E. huxleyi* under oceanic conditions where nitrate was replete but phosphate was less than 0.3 μM (Riegman et al. 2000). Also, the high affinity of *E. huxleyi* for phosphate has been successfully used as the experimental basis for a model of its distribution in the NE Atlantic (Tyrrell and Taylor 1996).

Effects of irradiance on *E. huxleyi* physiology

In our study, increasing the irradiance level greatly promoted the growth and photosynthetic rates of *E. huxleyi* below the saturation point. Some previous studies on Northern Hemisphere *E. huxleyi* strains observed a higher saturating irradiance for *E. huxleyi* growth than other phytoplankton groups, even at > 300 μmol photons m^{-2} s^{-1} depending on the incubation temperature (Nanninga and Tyrrell 1996; Paasche 1999). In comparison, the present study suggested a lower saturation irradiance of $\sim$100 μmol photons m^{-2} s^{-1} for growth and photosynthesis at 14°C, and photo-inhibition was only found at the highest irradiance tested (650 μmol photons m^{-2} s^{-1}) for both growth and photosynthesis.

Interestingly, the calcification rate of *E. huxleyi* in the present study was saturated at a lower irradiance than that for both growth and photosynthesis, with photo-inhibition of calcification also observed at the lower irradiance of 350 μmol photons m^{-2} s^{-1}. Similarly, a study on Northern Hemisphere *E. huxleyi* strain 88E found that calcification was less light dependent than photosynthesis with calcification observed in the dark at 15°C and 20°C (Nimer and Merrett 1993). The differential dependency on irradiance between calcification and photosynthesis might be due to the discrepancy in energy requirements of the two processes. The photon cost for calcification is considered to be 30% of that for photosynthesis as calculated by Anning et al. (1996) and even as low as 19% according to Raven and Crawfurd (2012). Previous studies provide evidence that the *E. huxleyi* calcification process is regulated indirectly by irradiance via the supporting energy from cyclic phosphorylation

generated in photosystem I (PSI) but not PSII (Paasche 1966b), and is dependent on the blue-light effects on HCO$_3^-$ transportation (Paasche 1966a, 2002; Anderson 2005). This mechanism of calcification regulation by irradiance indicates that the possibility of direct energetic limitation on calcification by irradiance is less likely compared with photosynthesis. Many studies have found a conspicuous dark calcification in short-term ^{14}C incubation (Paasche 1966b; Balch et al. 1992; Nimer and Merrett 1992). This may explain the higher calcification rate at low irradiances leading to significantly higher Cal : Photo ratio at the two lowest levels of 14 μmol photons m^{-2} s^{-1} and 40 μmol photons m^{-2} s^{-1} in our study. These findings also indicate that, with the shoaling of the mixed layer in the predicted future marine environment, the calcification process is likely to be weakened more than photosynthesis in *E. huxleyi* cells under increased irradiance, and thus lead to a decrease in inorganic carbon to organic carbon production by this species.

Effects of temperature on *E. huxleyi* physiology

Temperature is an important factor controlling the metabolic rates of marine phytoplankton (Raven and Geider 1988). In the present study, the southern hemisphere temperate strain of *E. huxleyi* was able to grow across a temperature gradient of 21°C (4–25°C). Compared to other coccolithophore species, *E. huxleyi* is considered to be a *r*-selected species with higher growth rates (Fagerbakke et al. 1994); therefore, it has been found in the ocean globally, with a wide temperature range of 1–30°C (Winter et al. 1994). However, in the present study *E. huxleyi* cells grew much more slowly at the lowest temperatures of 4°C and 7°C, compared to other treatments. It has been suggested that the wide distribution of *E. huxleyi* is caused by the existence of temperature-selected ecotypes (Paasche 2002). A survey of Southern Ocean surface water coccolithophore distributions from 2001 to 2006 (Cubillos et al. 2007) found the *E. huxleyi* morphotype A was only observed north of the Polar Front, while the other morphotype B/C (less calcified) mainly dominated in the colder region (south of the Polar Front). In line with Cubillos et al. (2007), the observed growth suppression of the *E. huxleyi* morphotype A at low temperatures in our study indicates that its ability to adapt to low temperature conditions may be limited; and thus the morphotype A is likely to be out-competed by other *E. huxleyi* morphotypes in the sub-polar or polar regions. On the other hand, previous study has suggested that the calcification of *E. huxleyi* morphotype B/C might be more sensitive to the change in seawater carbonate chemistry (Müller et al. 2015). As such, the PIC production of *E. huxleyi* populations in the cold sub-polar/polar regions might be weakened more by the future trend of ocean acidification than the temperate regions.

In the present study, the optimal temperature for calcification was lower than that for photosynthesis. This led to a

significantly lower Cal : Photo ratio at 25°C compared to that at 15°C, and yielded an optimal temperature of ~17°C for the Cal : Photo ratio. Interestingly, the temperature optimum for calcification was closer to the temperature (14°C) of the stock culture in our study, and lower than that for growth or photosynthesis, as also reported for the Northern Hemisphere *E. huxleyi* strain BT-6 by Watabe and Wilbur (1966). Based on these findings, it can be speculated that with the 2–6°C warming in the future ocean, the calcification process of *E. huxleyi* is likely to be impaired while photosynthesis will be favored and lead to a lower Cal : Photo ratio and a reduced rain ratio (Rost and Riebesell 2004).

In addition to the Cal : Photo ratio, the morphology of the coccoliths can also be affected by temperature. In the present study, along with the significant decrease in Cal : Photo ratio at 4°C and 7°C, there was also a greater occurrence of severely malformed coccoliths with incomplete distal shield elements at these lower temperatures. This malformation might be a consequence of the mismatch between cell growth and crystal formation at low temperatures (Watabe and Wilbur 1966) and lower tolerance of calcite formation to low temperature than photosynthesis. However, despite of the obvious coccolith malformation and low calcification rates at the two lowest temperature treatments, the cellular particulate inorganic carbon content was not significantly decreased in our study (Feng 2015; Feng et al. unpubl.). This can probably be attributed to the larger cell size at low temperature (data not shown). Similarly, by examining the malformation of coccoliths of several *E. huxleyi* strains under different CO_2 concentrations, Langer et al. (2011) also suggests a lack of correlation between morphology and calcification/accumulated cellular calcite.

Effects of CO_2 on *E. huxleyi* physiology

The effects of rising pCO_2 on the physiology of *E. huxleyi*, especially on calcification, have received increasing attention during the last decade due to the sensitivity of calcification to seawater carbonate chemistry change (e.g., Riebesell et al. 2000; Iglesias-Rodriguez et al. 2008). However, the results of the many studies from a wide range of *E. huxleyi* isolates and environmental conditions (Table 1) suggest no significant group-specific response patterns in the physiological sensitivity of *E. huxleyi* to altered pCO_2.

In the present study, rising pCO_2 slightly decreased calcification and the Cal : Photo ratio, but had no significant effect on either the photosynthetic or growth rate during the steady-state growth phase. *E. huxleyi* has a functional CCM, utilizing HCO_3^- as inorganic carbon source by active transport or by catalyzed dehydration and diffusion of CO_2 (Kottmeier et al. 2016). This explains that the growth of *E. huxleyi* in our study was able to acclimate to pCO_2 as low as 8 Pa after 16 d' of incubation. Carbonic anhydrase (CA) is present in the chloroplasts of *E. huxleyi* cells, and may convert HCO_3^- to CO_2 at the site of carbon fixation (Nimer et al.

1994, 1997). Although *E. huxleyi* coccolith-bearing C-cells may lack external CA under exponential growth, studies suggested that the external CA of the high-calcifying Northern Hemisphere *E. huxleyi* strain 88E was activated under low DIC concentrations (Nimer and Merrett 1996). More recent work on functional gene expression of *E. huxleyi* strain B92/11 observed that three of the five CAs measured (including both external and internal CAs) were up-regulated at low pCO_2 after > 7 generations of acclimation (Bach et al. 2013). Similarly, for a northern hemisphere *E. huxleyi* strain RCC1256 and three other coccolithophore species, the growth was not suppressed under DIC concentration as low as 2 mmol kg^{-1} (267 μatm), compared to higher pCO_2 treatments at steady pH (Hermoso et al. 2016). Hence, increased activity of CAs may also be the case in the present study for a Southern Hemisphere strain, explaining the acclimation of *E. huxleyi* growth to low pCO_2 conditions and the lack of an effect of pCO_2 on photosynthetic rate.

The growth rate of *E. huxleyi* during the steady-state growth phase decreased slightly at high pCO_2 in our study, and there was an even greater decrease in the calcification rate with rising pCO_2. Based on the literature and the summary presented in Table 1, these trends may be caused by the effects of increasing proton (H^+) concentration on cellular pH homeostasis at high pCO_2 (Riebesell and Tortell 2011). Specifically, due to the presence of a H^+ permeable pathway located on the *E. huxleyi* plasma membrane, the intracellular pH of *E. huxleyi* may decrease linearly with decreasing extracellular pH and increasing HCO_3^- concentration in the medium (Suffrian et al. 2011), i.e., increasing pCO_2 in our study. Therefore, intracellular acidification may require more energy to counteract cytosol acidification by neutralizing the H^+ generated from calcification (Nimer and Merrett 1993; Hermoso 2015), leading to the decreased calcification observed in the present study, especially at the highest pCO_2.

Our study observed a linear decrease in Cal : Photo ratio with rising pCO_2. Calcification was hypothesized to be coupled with photosynthesis, as the CO_2 or H^+ produced in calcification may be used as substrate for photosynthesis and for uncatalyzed dehydration of the internal pool of HCO_3^-, respectively, in order to minimize energy expenditure during active CCM (Giordano et al. 2005; Gussone et al. 2006; Ziveri et al. 2007). However, recent studies provide new evidence that there is no absolute linkage between the two processes, as *E. huxleyi* photosynthesis was not affected when calcification rates were weakened at very low Ca^{2+} concentrations (Trimborn et al. 2007; Leonardos et al. 2009). According to the above findings, it is assumed that more photosynthetically derived energy must be relocated to maintain the trans-plasmalemma electrical potential difference (determined by the pH gradient) in order to pump out the extra H^+ generated in calcification at high pCO_2 (Raven 2011; Ries 2011; Taylor et al. 2011), leaving less energy

available for calcification. This might be the case in our study, leading to decreased Cal : Photo ratio at higher $p\mathrm{CO_2}$.

The calcification rate was slightly lower at $p\mathrm{CO_2}$ 8 Pa than that at 15 Pa or 39 Pa in our study, which was likely to be linked with the lower $\mathrm{HCO_3^-}$ availability. In addition to changes in ambient $\mathrm{CO_2}$ and $\mathrm{H^+}$ concentrations, rising $p\mathrm{CO_2}$ also results in an increasing $\mathrm{HCO_3^-}$ concentration (Caldeira and Wickett 2003). This may also affect *E. huxleyi* calcification as $\mathrm{HCO_3^-}$ serves as the sole inorganic substrate for calcification (Paasche 2002; Raven and Crawfurd 2012). Incubation experiments conducted under a wide range of inorganic carbon concentrations suggested that the calcification rate of *E. huxleyi* was regulated by the $\mathrm{HCO_3^-}$ concentration in the medium, but not the ambient $\mathrm{CO_2}$ concentration (Bach et al. 2013, Table 1). However, the present study was conducted using a DIC manipulation method ($\mathrm{CO_2}$ bubbling) to mimic changes projected in the marine environment; therefore it cannot dissect the differential effects on *E. huxleyi* of each seawater carbonate species (Hurd et al. 2009). In spite of the increase in $\mathrm{HCO_3^-}$ concentration with increasing $p\mathrm{CO_2}$, both the calcification rate and Cal : Photo ratio decreased probably due to the effects of increasing $\mathrm{H^+}$ concentration in our study, as described earlier.

The genotypic difference between various *E. huxleyi* strains (Langer et al. 2009; Beaufort et al. 2011; Read et al. 2013) is thought to be one of the causes of the variety of responses of *E. huxleyi* calcification to $\mathrm{CO_2}$ concentration, reported by numerous studies (see Table 1 for northern and southern hemisphere strains). Studies on three Southern Ocean *E. huxleyi* ecotypes/morphotypes indicate that there are genetic differences between different morphotypes (Cook et al. 2011). In a study on Southern Hemisphere *E. huxleyi* strains by Müller et al. (2015), they reported that the calcification of morphotype B/C was weakened more, with increasing $p\mathrm{CO_2}$, than that of morphotype A. Hence, the differential sensitivity of different morphotypes in response to OA may probably explain the differences in PIC/calcification responses between our study and some other published results (Table 1). For example, in our study, the calcification rate of *E. huxleyi* morphotype A only decreased slightly when $p\mathrm{CO_2}$ increased from 39 Pa to 74 Pa (statistically non-significant); however, the cellular PIC content of a morphotype B/C (Northern Hemisphere strain CCMP 371) decreased by 50% when $p\mathrm{CO_2}$ changed within the same range (Feng et al. 2008). These observations are also in line with the strain-specific responses of *E. huxleyi* to changing seawater carbonate chemistry examined by Langer et al. (2009). In their study, *E. huxleyi* morphotype A strains RCC1238 and RCC1256 showed only little or non-significant changes in PIC/POC productions when $p\mathrm{CO_2}$ rose from 200 ppm to 1000 ppm; while the ratio significantly decreased for morphotype B strain RCC1212 with rising $p\mathrm{CO_2}$ (Table 1).

Furthermore, the energy-dependent calcification response to $\mathrm{CO_2}$ may be regulated by other environmental drivers
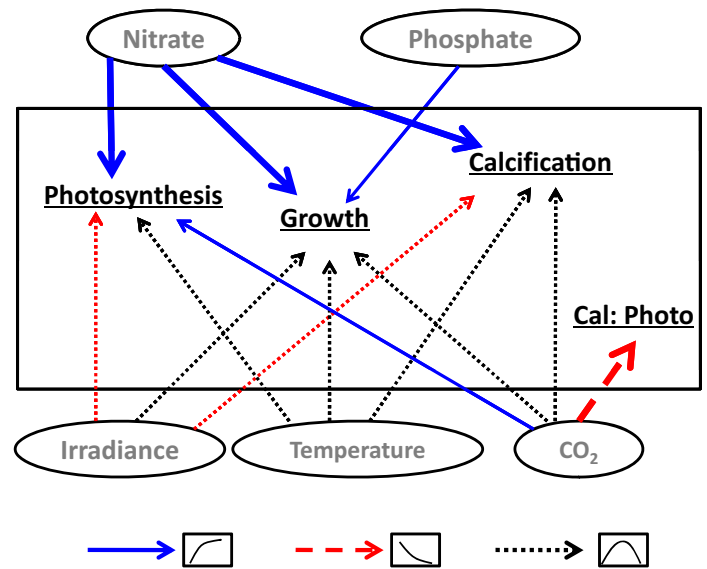
Fig. 7. Conceptual model of the specific effects of each the five environmental drivers, within the examined ranges in this study, on the physiological rate processes and biogeochemical ratios of *E. huxleyi*. ***The box denotes the *E. huxleyi* cell. Different arrow types and colors indicate the different regulation norms as illustrated in the three squares below the figure. Arrows in bold indicate the environmental drivers that play the most important role regulating the connected physiological metrics under the predicted environmental conditions for the year 2100. [Color figure can be viewed at wileyonlinelibrary.com]

(Raven and Crawfurd 2012) such as irradiance, temperature, and nutrient availability; thus these environmental conditions may regulate the calcification response to $p\mathrm{CO_2}$. Feng et al. (2008) reported that the cellular PIC content of *E. huxleyi* strain CCMP 371 was not significantly affected by $p\mathrm{CO_2}$ at an irradiance of 50 μmol photons $\mathrm{m^{-2}\,s^{-1}}$, but significantly decreased by raising $p\mathrm{CO_2}$ at a higher irradiance of 400 μmol photons $\mathrm{m^{-2}\,s^{-1}}$. The present $\mathrm{CO_2}$ manipulation experiment was conducted at a temperature of 14°C and irradiance of 140 μmol photons $\mathrm{m^{-2}\,s^{-1}}$, the conditions at which the stock cultures were maintained and to which they would have acclimated. Our results indicate that changes in nitrate concentration, irradiance and temperature can all significantly affect the calcification rate of the Southern Hemisphere *E. huxleyi* strain. Therefore, the physiological response of *E. huxleyi* to change in $p\mathrm{CO_2}$ would probably be different at other combinations of irradiance, temperature, and nitrate levels.

Future predictions of *E. huxleyi* physiology responses to environmental changes

The present study is able to tease apart the effect that each environmental driver plays on the growth, photosynthetic, and calcification rates, as shown in the conceptual model (Fig. 7). Given that all the three rate processes are central processes in *E. huxleyi* physiology, and the Cal : Photo ratio has implications in the marine carbon cycle

(Rost and Riebesell 2004), these findings will help improve our understanding of how growth, photosynthesis, and calcification will respond to any future changes in the marine environment and how the consequent marine carbon cycle will be affected by the changes in *E. huxleyi* physiology. The results suggest that the predicted reduction of nitrate concentration by 2100 in the Chatham Rise area may result in a decrease in the growth, photosynthetic and calcification rates of *E. huxleyi* strain NIWA1108, with the change in nitrate concentration playing the most important role in regulating these physiological rates compared to the other four environmental drivers tested here. Temperature plays the second most important role in regulating the growth and photosynthesis of *E. huxleyi* by increasing both growth and photosynthetic rates. Moreover, rising pCO_2 ranks second in importance in regulating calcification, by decreasing the calcification rate. Rising pCO_2 will also decrease the Cal : Photo ratio of *E. huxleyi*, and is ranked as the most important driver controlling this ratio.

Our study provides evidence of the differential effects on *E. huxleyi* physiological rate processes by changes various environmental drivers; and thus the interplay between these drivers may amplify or offset the effects of individual drivers, that is, having synergistic/antagonistic interactions as described in Folt et al. (1999). In the future marine environment, marine phytoplankton will be subjected to complex simultaneous changes of multiple environmental drivers (Boyd et al. 2010, 2015, 2016; Boyd and Hutchins 2012). For the future Chatham Rise area, based on our results, the projected decrease in nitrate concentration will decrease the growth, photosynthetic and calcification rates of *E. huxleyi* by 20–25%. In contrast, warming will increase the three rates by 11–15%. This increase may offset the decrease in the rates due to decrease in nitrate concentration by roughly ~50% in the future marine environment. On the other hand, rising pCO_2 (OA) itself will decrease the calcification rate by ~12%, which may reinforce the effects of decreased nitrate (Feng 2015; Feng et al. unpubl.). Therefore, the interplay between the multiple environmental drivers may have complex interactive effects on the physiology of *E. huxleyi*, and these interactions are probably more dramatic than the additive effects of the single drivers examined in the present study (Feng 2015). Furthermore, due to the importance nitrate concentration plays in all three rate processes for the *E. huxleyi* examined in our study, we speculate that the nitrate availability may also be the determining factor when studying the interactions between multiple drivers (Brennan and Collins 2015; Feng et al. unpubl.). However, the available published relevant manipulation experiments on *E. huxleyi* are largely focused on a single environmental driver, mainly the effects of OA (Gattuso and Hansson 2011). Therefore, further study on the complex interplay among the multiple environmental drivers will be a necessary addition to our knowledge to determine how this ecologically important species will respond to the concurrent changes in the multiple environmental conditions and its consequent biogeochemical feedbacks (Feng et al. unpubl.).

The ranking in our study also indicates the importance of the scale of changes in the environmental drivers on *E. huxleyi* physiological rate processes. For instance, although changes in both irradiance and temperature significantly affected the growth, photosynthesis, and calcification rates of *E. huxleyi* within the range examined in the present study, neither driver played the most important role in regulating growth, photosynthesis or calcification based on future predictions for year 2100. This may be due to the small predicted future (2100) changes for these two drivers in the Chatham Rise. In the present study, irradiance was increased by 25% from 140 μmol photons m^{-2} s^{-1} to 175 μmol photons m^{-2} s^{-1}. Similarly, there was only a 2°C predicted increase in temperature (from 14°C to 16°C) which led to smaller changes in growth, photosynthetic, and calcification rates than decreasing nitrate concentration. Therefore, the magnitude of predicted shifts in environmental conditions will also be an important factor when making predictions for future changes in *E. huxleyi* physiology in different regions.

In summary, this study provides evidence that, although OA may play the most important role in controlling the Cal : Photo ratio of *E. huxleyi* under the predicted future conditions for 2100 in the Chatham Rise area, other environmental drivers, such as nitrate concentration, play an even more influential role in regulating the growth, photosynthesis, and calcification rates. This further stresses the importance of considering other environmental drivers in addition to OA when examining the physiological responses of *E. huxleyi* to future environmental change.

References

Anderson, T. R. 2005. Plankton functional type modelling: Running before we can walk? J. Plankton Res. **27**: 1073–1081. doi:10.1093/plankt/fbi076

Anning, T., N. Nimer, M. J. Merrett, and C. Brownlee. 1996. Costs and benefits of calcification in coccolithophorids. J. Mar. Syst. **9**: 45–56. doi:10.1016/0924-7963(96)00015-2

Arrigo, K. R. 2005. Marine microorganisms and global nutrient cycles. Nature **437**: 349–355. doi:10.1038/nature04159

Bach, L. T., L. C. Mackinder, K. G. Schulz, G. Wheeler, D. C. Schroeder, C. Brownlee, and U. Riebesell. 2013. Dissecting the impact of CO_2 and pH on the mechanisms of photosynthesis and calcification in the coccolithophore *Emiliania huxleyi*. New Phytol. **199**: 121–134. doi:10.1111/nph.12225

Balch, W. M., P. M. Holligan, and K. A. Kilpatrick. 1992. Calcification, photosynthesis and growth of the bloom-forming coccolithophore, *Emiliania huxleyi*. Cont. Shelf Res. **12**: 1353–1374. doi:10.1016/0278-4343(92)90059-s

Balch, W. M., D. T. Drapeau, B. C. Bowler, E. Lyczskowski, E. S. Booth, and D. Alley. 2011. The contribution of

coccolithophores to the optical and inorganic carbon budgets during the Southern Ocean Gas Exchange Experiment: New evidence in support of the "Great Calcite Belt" hypothesis. J. Geophys. Res. Oceans **116**: C00F06. doi: 10.1029/2011JC006941

Barry, S., and J. Elith. 2006. Error and uncertainty in habitat models. J. Appl. Ecol. **43**: 413–423. doi:10.1111/j.1365-2664.2006.01136.x

Beaufort, L., and others. 2011. Sensitivity of coccolithophores to carbonate chemistry and ocean acidification. Nature **476**: 80–83. doi:10.1038/nature10295

Blank, G. S., D. H. Robinson, and C. W. Sullivan. 1986. Diatom mineralization of silicic acid. VIII. Metabolic requirements and the timing of protein synthesis. J. Phycol. **22**: 382–389. doi: 10.1111/j.1529-8817.1986.tb00039.x

Bopp, L., P. Monfray, O. Aumont, J.-L. Dufresne, H. Le Treut, G. Madec, L. Terray, and J. C. Orr. 2001. Potential impact of climate change on marine export production. Global Biogeochem. Cy. **15**: 81–99. doi:10.1029/1999gb001256

Boyd, P. W., J. Laroche, M. Gall, R. Frew, and R. M. L. Mckay. 1999. Role of iron, light, and silicate in controlling algal biomass in subantarctic waters SE of New Zealand. J. Geophys. Res. (C Oceans) **104**: 13395–13408. doi: 10.1029/1999jc900009

Boyd, P. W., and S. C. Doney. 2002. Modelling regional responses by marine pelagic ecosystems to global climate change. Geophys. Res. Lett. **29**. doi:10.1029/2001gl014130

Boyd, P. W., R. Strzepek, F. Fu, and D. A. Hutchins. 2010. Environmental control of open-ocean phytoplankton groups: Now and in the future. Limnol. Oceanogr. **55**: 1353–1376. doi:10.4319/lo.2010.55.3.1353

Boyd, P. W., and C. S. Law. 2011. A climate change atlas for the New Zealand exclusive economic zone. National Institute of Water and Atmosphere (NIWA) Information Series.

Boyd, P. W., and D. A. Hutchins. 2012. Understanding the responses of ocean biota to a complex matrix of cumulative anthropogenic change. Mar. Ecol. Prog. Ser. **470**: 125–135. doi:10.3354/meps10121

Boyd, P. W., S. T. Lennartz, D. M. Glover, and S. C. Doney. 2015. Biological ramifications of climate-change-mediated oceanic multi-stressors. Nat. Clim. Chang. **5**: 71–79. doi:10.1038/nclimate2441

Boyd, P. W., and others. 2016. Physiological responses of a Southern Ocean diatom to complex future ocean conditions. Nat. Clim. Chang. **6**: 207–213. doi:10.1038/nclimate2811

Brennan, G., and S. Collins. 2015. Growth responses of a green alga to multiple environmental drivers. Nat. Clim. Chang. **5**: 892–897. doi:10.1038/nclimate2682

Buitenhuis, E. T., H. J. W. de Baar, and M. J. W. Veldhuis. 1999. Photosynthesis and calcification by *Emiliania huxleyi*

(Prymnesiophyceae) as a function of inorganic carbon species. J. Phycol. **35**: 949–959. doi:10.1046/j.1529-8817.1999.3550949.x

Caldeira, K., and M. E. Wickett. 2003. Anthropogenic carbon and ocean pH. Nature **425**: 365–365. doi:10.1038/425365a

Cook, S. S., L. Whitlock, S. W. Wright, and G. M. Hallegraeff. 2011. Photosynthetic pigment and genetic differences between two southern ocean morphotypes of *Emiliania huxleyi* (Haptophyta). J. Phycol. **47**: 615–626. doi:10.1111/j.1529-8817.2011.00992.x

Cubillos, J. C., S. W. Wright, G. Nash, M. F. de Salas, B. Griffiths, B. Tilbrook, A. Poisson, and G. M. Hallegraeff. 2007. Calcification morphotypes of the coccolithophorid *Emiliania huxleyi* in the Southern Ocean: Changes in 2001 to 2006 compared to historical data. Mar. Ecol. Prog. Ser. **348**: 47–54. doi:10.3354/meps07058

De Bodt, C., N. Van Oostende, J. Harlay, K. Sabbe, and L. Chou. 2010. Individual and interacting effects of pCO_2 and temperature on *Emiliania huxleyi* calcification: study of the calcite production, the coccolith morphology and the coccosphere size. Biogeosciences **7**: 1401–1412. doi:10.5194/bg-7-1401-2010

Dickson, A. G., and F. J. Millero. 1987. A comparison of the equilibrium-constants for the dissociation of carbonic-acid in seawater media. Deep-Sea Res. **34**: 1733–1743. doi:10.1016/0198-0254(88)92460-0

Dickson, A. G., C. L. Sabine, and J. R. Christian. 2007. Guide to best practices for ocean CO_2 measurements. North Pacific Marine Science Organization.

Engel A., and others. 2005. Testing the direct effect of CO_2 concentration on a bloom of the coccolithophorid *Emiliania huxleyi* in mesocosm experiments. Limnol. Oceanogr. **50**: 493–507. doi:10.4319/lo.2005.50.2.0493

Fagerbakke, K. M., M. Heldal, S. Norland, B. R. Heimdal, and H. Batvik. 1994. *Emiliania huxleyi* chemical composition and size of coccoliths from enclosure experiments and a Norwegian fjord. Sarsia **79**: 349–355. doi:10.1080/00364827.1994.10413566

Falkowski, P. G., M. E. Katz, A. H. Knoll, A. Quigg, J. A. Raven, O. Schofield, and F. J. R. Taylor. 2004. The evolution of modern eukaryotic phytoplankton. Science **305**: 354–360. doi:10.1126/science.1095964

Feng, Y. 2015. Environmental controls on the physiology of marine coccolithophore *Emiliania huxleyi* strain NIWA 1108. Ph.D. thesis. Univ. of Otago.

Feng, Y., M. E. Warner, Y. Zhang, J. Sun, F. X. Fu, J. M. Rose, and D. A. Hutchins. 2008. Interactive effects of increased pCO_2, temperature and irradiance on the marine coccolithophore *Emiliania huxleyi* (Prymnesiophyceae). Eur. J. Phycol. **43**: 87–98. doi:10.1080/09670260701664674

Feng, Y., and others. 2009. Effects of increased pCO_2 and temperature on the North Atlantic spring bloom: I. The phytoplankton Community and Biogeochemical

Response. Mar. Ecol. Progr. Ser. **388**: 13–25. doi:10.3354/meps08133

Findlay, H. S., P. Calosi, and K. Crawfurd. 2011. Determinants of the PIC:POC response in the coccolithophore *Emiliania huxleyi* under future ocean acidification scenarios. Limnol. Oceanogr. **56**: 1168–1178. doi:10.4319/lo.2011.56.3.1168

Fiorini, S., J. J. Middelburg, and J. P. Gattuso. 2011. Testing the effects of elevated pCO_2 on coccolithophores (Prymnesiophyceae): comparison between haploid and diploid life stages. J. Phycol. **47**: 1281–1291. doi:10.1111/j.1529-8817.2011.01080.x

Folt, C. L., C. Y. Chen, M. V. Moore, and J. Burnaford. 1999. Synergism and antagonism among multiple stressors. Limnol. Oceanogr. **44**: 864–877. doi:10.4319/lo.1999.44.3_part_2.0864

Frigeri, L. G., T. R. Radabaugh, P. A. Haynes, and M. Hildebrand. 2006. Identification of proteins from a cell wall fraction of the diatom *Thalassiosira pseudonana*: Insights into silica structure formation. Mol. Cell. Proteomics **5**: 182–193. doi:10.1074/mcp.M500174-MCP200

Gabriel, W., and M. Lynch. 1992. The selective advantage of reaction norms for environmental tolerance. J. Evol. Biol. **5**: 41–59. doi:10.1046/j.1420-9101.1992.5010041.x

Gattuso, J. P., and L. Hansson. 2011. Ocean acidification. Oxford Univ. Press.

Gilbert, M., A. Domin, A. Becker, and C. Wilhelm. 2000. Estimation of primary productivity by chlorophyll *a* in vivo fluorescence in freshwater phytoplankton. Photosynthetica **38**: 111–126. doi:10.1023/A:1026708327185

Giordano, M., J. Beardall, and J. A. Raven. 2005. CO_2 concentrating mechanisms in algae: Mechanisms, environmental modulation, and evolution. Annu. Rev. Plant Biol. **56**: 99–131. doi:10.1146/annurev.arplant.56.032604.144052

Guillard, R. R., and J. H. Ryther. 1962. Studies of marine planktonic diatoms.1. Cyclotella nana (Hustet), and *Detonula confevacea* (Cleve Gran). Can. J. Microbiol. **8**: 229–239. doi:10.1139/m62-029

Gussone, N., G. Langer, S. Thoms, G. Nehrke, A. Eisenhauer, U. Riebesell, and G. Wefer. 2006. Cellular calcium pathways and isotope fractionation in *Emiliania huxleyi*. Geology **34**: 625–628. doi:10.1130/g22733.1

Henderiks, J., A. Winter, M. Elbrächter, R. Feistel, A. van der Plas, G. Nausch, and R. Barlow. 2012. Environmental controls on *Emiliania huxleyi* morphotypes in the Benguela coastal upwelling system (SE Atlantic). Mar. Ecol. Prog. Ser. **448**: 51–66. doi:10.3354/meps09535

Hermoso, M. 2015. Control of ambient pH on growth and stable isotopes in planktonic calcifying algae. Paleoceanography **30**: 1100–1112. doi:10.1002/2015PA002844

Hermoso, M., I. Z. Chan, H. L. Mcclelland, A. M. Heureux, and R. E. Rickaby. 2016. Vanishing coccolith vital effects with alleviated carbon limitation. Biogeosciences **13**: 301–312. doi:10.5194/bg-13-301-2016

Holligan, P. M., M. Viollier, D. S. Harbour, P. Camus, and M. Champagnephilippe. 1983. Satellite and ship studies of coccolithophore production along a continetal-shelf edge. Nature **304**: 339–342. doi:10.1038/304339a0

Holligan, P. M., and others. 1993. A biogeochemical study of the coccolithophore, *Emiliania huxleyi*, in the North Atlantic. Global Biogeochem. Cycles **7**: 879–900. doi:10.1029/93gb01731

Honisch, B., and others. 2012. The geological record of ocean acidification. Science **335**: 1058–1063. doi:10.1126/science.1208277

Hoppe, C. J. M., G. Langer, and B. Rost. 2011. *Emiliania huxleyi* shows identical responses to elevated pCO_2 in TA and DIC manipulations. J. Exp. Mar. Biol. Ecol. **406**: 54–62. doi:10.1016/j.jembe.2011.06.008

Hurd, C. L., C. D. Hepburn, K. I. Currie, J. A. Raven, and K. A. Hunter. 2009. Testing the effects of ocean acidification on algal metabolism: Considerations for experimental designs. J. Phycol. **45**: 1236–1251. doi:10.1111/j.1529-8817.2009.00768.x

Iglesias-Rodriguez, M. D., O. M. Schofield, J. Batley, L. K. Medlin, and P. K. Hayes. 2006. Intraspecific genetic diversity in the marine coccolithophore *Emiliania huxleyi* (Prymnesiophyceae): The use of microsatellite analysis in marine phytoplankton population studies. J. Phycol. **42**: 526–536. doi:10.1111/j.1529-8817.2006.00231.x

Iglesias-Rodriguez, M. D., and others. 2008. Phytoplankton calcification in a high-CO_2 world. Science **320**: 336–340. doi:10.1126/science.1154122

Kottmeier, D. M., S. D. Rokitta, and B. Rost. 2016. Acidification, not carbonation, is the major regulator of carbon fluxes in the coccolithophore *Emiliania huxleyi*. New Phytol. **211**: 126–37. doi: 10.1111/nph.13885

Langer, G. 2011. CO_2 mediation of adverse effects of seawater acidification in *Calcidiscus leptoporus*. Geochem. Geophys. Geosyst. **12**: Q05001. doi:10.1029/2010gc003393

Langer, G., M. Geisen, K. H. Baumann, J. Kläs, U. Riebesell, S. Thoms, and J. R. Young. 2006. Species-specific responses of calcifying algae to changing seawater carbonate chemistry. Geochem. Geophys. Geosyst. **7**: Q09006. doi:10.1029/2005gc001227

Langer, G., and I. Benner. 2009. Effect of elevated nitrate concentration on calcification in *Emiliania huxleyi*. J. Nannoplankton Res. **30**: 77–80.

Langer, G., G. Nehrke, I. Probert, J. Ly, and P. Ziveri. 2009. Strain-specific responses of *Emiliania huxleyi* to changing seawater carbonate chemistry. Biogeosciences **6**: 2637–2646. doi:10.5194/bg-6-2637-2009

Langer, G., I. Probert, G. Nehrke, and P. Ziveri. 2011. The morphological response of *Emiliania huxleyi* to seawater carbonate chemistry changes: An inter-strain comparison. J. Nannoplankton Res. **32**: 29–34.

Lefebvre, S. C., and others. 2012. Nitrogen source and pCO_2 synergistically affect carbon allocation, growth and

morphology of the coccolithophore *Emiliania huxleyi*: Potential implications of ocean acidification for the carbon cycle. Glob. Chang. Biol. **18**: 493–503. doi:10.1111/j.1365-2486.2011.02575.x

Leonardos, N., B. Read, B. Thake, and J. R. Young. 2009. No mechanistic dependence of photosynthesis on calcification in the coccolithophorid *Emiliania huxleyi* (Haptophyta). J. Phycol. **45**: 1046–1051. doi:10.1111/j.1529-8817.2009.00726.x

Litchman, E. 2000. Growth rates of phytoplankton under fluctuating light. Freshw. Biol. **44**: 223–235. doi:10.1046/j.1365-2427.2000.00559.x

Mackinder, L., G. Wheeler, D. Schroeder, P. Von Dassow, U. Riebesell, and C. Brownlee. 2011. Expression of biomineralization-related ion transport genes in *Emiliania huxleyi*. Environ. Microbiol. **13**: 3250–3265. doi:10.1111/j.1462-2920.2011.02561.x

Marsh, M. E. 1994. Polyanion-mediated mineralization-assembly and reorganization of acidic polysaccharide in the Golgi system of a coccolithophorid alga during mineral deposition. Protoplasma. **177**: 108–122. doi:10.1007/BF01378985

Mcgraw, C. M., C. E. Cornwall, M. R. Reid, K. I. Currie, C. D. Hepburn, P. Boyd, C. L. Hurd, and K. A. Hunter. 2010. An automated pH-controlled culture system for laboratory-based ocean acidification experiments. Limnol. Oceanogr.: Methods **8**: 686–694. doi:10.4319/lom.2010.8.686

Megard, R. O., D. W. Tonkyn, and W. H. Senft. 1984. Kinetics of oxygenic photosynthesis in planktonic algae. J. Plankton Res. **6**: 325–337. doi:10.1093/plankt/6.2.325

Mehrbach, C., C. H. Culberson, J. E. Hawley, R. M. Pytkowic. 1973. Measurement of apparent dissociation cosntants of carbonic acid in seawater at atmospheric pressure. Limnol. Oceanogr. **18**: 897–907. doi:10.4319/lo.1973.18.6.0897

Michaelis, L., and M. L. Menten. 1913. Die kinetik der invertinwirkung. Biochem. Z. **49**: 333–369.

Milliman, J. D. 1993. Production and accumulation of calcium carbonate in the ocean: Budget of nonsteady state. Global Biogeochem. Cy. **7**: 927–957. doi:10.1029/93gb02524

Moore, T. S., M. D. Dowell, and B. A. Franz. 2012. Detection of coccolithophore blooms in ocean color satellite imagery: A generalized approach for use with multiple sensors. Remote Sens. Environ. **117**: 249–263. doi:10.1016/j.rse.2011.10.001

Müller, M. N., K. G. Schulz, and U. Riebesell. 2010. Effects of long-term high CO_2 exposure on two species of coccolithophores. Biogeosciences **7**: 1109–1116. doi:10.5194/bg-7-1109-2010

Müller, M. N., T. W. Trull, and G. M. Hallegraeff. 2015. Differing responses of three Southern Ocean *Emiliania huxleyi* ecotypes to changing seawater carbonate chemistry. Mar. Ecol. Prog. Ser. **531**: 81–90. doi:10.3354/meps11309

Nanninga, H. J., and T. Tyrrell. 1996. Importance of light for the formation of algal blooms by *Emiliania huxleyi*. Mar. Ecol. Prog. Ser. **136**: 195–203. doi:10.3354/meps136195

Nimer, N. A., and M. J. Merrett. 1992. Calcification and utilization of inorganic carbon by the coccolithophorid *Emiliania huxleyi* Lohmann. New Phytol. **121**: 173–177. doi:10.1111/j.1469-8137.1992.tb01102.x

Nimer, N. A., and M. J. Merrett. 1993. Calcification rate in *Emiliania huxleyi* Lohmann in response to light, intrate and availability of inorganic carbon. New Phytol. **123**: 673–677. doi:10.1111/j.1469-8137.1993.tb03776.x

Nimer, N. A., Q. Guan, and M. J. Merrett. 1994. Extracellular and intracellular carbonic-anhydrase in relation to culture age in a high-calcifying strain of *Emiliania huxleyi* Lohmann. New Phytol. **126**: 601–607. doi:10.1111/j.1469-8137.1994.tb02954.x

Nimer, N. A., and M. J. Merrett. 1996. The development of a CO_2 concentrating mechanism in *Emiliania huxleyi*. New Phytol. **133**: 383–389. doi:10.1111/j.1469-8137.1996.tb01905.x

Nimer, N. A., M. D. Iglesiasrodriguez, and M. J. Merrett. 1997. Bicarbonate utilization by marine phytoplankton species. J. Phycol. **33**: 625–631. doi:10.1111/j.0022-3646.1997.00625.x

Paasche, E. 1964. A tracer study of the inorganic carbon uptake during coccolith formation and photosynthesis in the coccolithophorid *Coccolithus huxleyi*. Physiologia Plantarum Suppl. **3**: 1–82.

Paasche, E. 1966a. Action spectrum of coccolith formation. Physiol. Plant. **19**: 770–779. doi:10.1111/j.1399-3054.1966.tb07062.x

Paasche, E. 1966b. Adjustment to light and dark rates of coccolith formation. Physiol. Plant. **19**: 271–278. doi:10.1111/j.1399-3054.1966.tb07017.x

Paasche, E. 1968. The effect of temperature, light intensity, and photoperiod on coccolith formation. Limnol. Oceanogr. **13**: 178–181. doi:10.4319/lo.1968.13.1.0178

Paasche, E. 1999. Reduced coccolith calcite production under light-limited growth: A comparative study of three clones of *Emiliania huxleyi* (Prymnesiophyceae). Phycologia. **38**: 508–516. doi:10.2216/i0031-8884-38-6-508.1

Paasche, E. 2002. A review of the coccolithophorid *Emiliania huxleyi* (Prymnesiophyceae), with particular reference to growth, coccolith formation, and calcification-photosynthesis interactions. Phycologia **40**: 503–529. doi:10.2216/i0031-8884-40-6-503.1

Paasche, E., and S. Brubak. 1994. Enhanced calcification in the coccolithophorid *Emiliania huxleyi* (Haptophyceae) under phosphorus limitation. Phycologia **33**: 324–330. doi:10.2216/i0031-8884-33-5-324.1

Paasche, E., S. Brubak, S. Skattebol, J. R. Young, and J. C. Green. 1996. Growth and calcification in the coccolithophorid *Emiliania huxleyi* (Haptophyceae) at low salinities. Phycologia **35**: 394–403. doi:10.2216/i0031-8884-35-5-394.1

Quigg, A., A. J. Irwin, and Z. V. Finkel. 2011. Evolutionary inheritance of elemental stoichiometry in phytoplankton. Proc. R. Soc. B Biol. Sci. **278**: 526–534. doi:10.1098/rspb.2010.1356

Raven, J. A. 2011. Effects on marine algae of changed seawater chemistry with increasing atmospheric CO_2. Biol. Environ. **111**: 1–17. doi:10.3318/bioe.2011.01

Raven, J. A., and R. J. Geider. 1988. Temperature and algal growth. New Phytol. **110**: 441–461. doi:10.1111/j.1469-8137.1988.tb00282.x

Raven, J., and others. 2005. Ocean acidification due to increasing atmospheric carbon dioxide. The Royal Society.

Raven, J. A., and K. Crawfurd. 2012. Environmental controls on coccolithophore calcification. Mar. Ecol. Prog. Ser. **470**: 137–166. doi:10.3354/meps09993

Read, B. A., and others. 2013. Pan genome of the phytoplankton *Emiliania* underpins its global distribution. Nature **499**: 209–213. doi:10.1038/nature12221

Redfield, A. C., B. H. Ketchum, and F. A. Richards. 1963. The influence of organisms on the composition of sea-water, p. 26–77 *In* M. N. Hill [ed.], The Sea. Ideas and observations on progress in the study of the seas. v2. The composition of sea-water. Comparative and descriptive oceanography. Interscience.

Riebesell, U., I. Zondervan, B. Rost, P. D. Tortell, R. E. Zeebe, and F. M. M. Morel. 2000. Reduced calcification of marine plankton in response to increased atmospheric CO_2. Nature **407**: 364–367. doi:10.1038/35030078

Riebesell, U., A. Koertzinger, and A. Oschlies. 2009. Sensitivities of marine carbon fluxes to ocean change. Proc. Natl. Acad. Sci. USA **106**: 20602–20609. doi:10.1073/pnas.0813291106

Riebesell, U., and P. D. Tortell. 2011. Effect of ocean acidification on pelagic organisms and ecosystems. Ocean acidification. Oxford Univ. Press.

Riegman, R., A. A. M. Noordeloos, and G. C. Cadee. 1992. Phaeocystis blooms and eutrophication of the continental coastal zones of the North Sea. Mar. Biol. **112**: 479–484. doi:10.1007/bf00356293

Riegman, R., W. Stolte, A. A. M. Noordeloos, and D. Slezak. 2000. Nutrient uptake, and alkaline phosphate (EC 3: 1: 3: 1) activity of *Emiliania huxleyi* (Prymnesiophyceae) during growth under N and P limitation in continuous cultures. J. Phycol. **36**: 87–96. doi:10.1046/j.1529-8817.2000.99023.x

Ries, J. B. 2011. A physicochemical framework for interpreting the biological calcification response to CO_2-induced ocean acidification. Geochim. Cosmochim. Acta. **75**: 4053–4064. doi:10.1016/j.gca.2011.04.025

Rokitta, S. D., and B. Rost. 2012. Effects of CO_2 and their modulation by light in the life-cycle stages of the coccolithophore *Emiliania huxleyi*. Limnol. Oceanogr. **57**: 607–618. doi:10.4319/lo.2012.57.2.0607

Rost, B., and U. Riebesell. 2004. Coccolithophores and the biological pump: Responses to environmental changes, p. 99–125 *In* H. R. Thierstein and J. R. Young [eds.], Coccolithophores: From molecular processes to global impact. Springer.

Rouco M., O. Branson, M. Lebrato, and M. D. Iglesias-Rodríguez. 2013. The effect of nitrate and phosphate availability on *Emiliania huxleyi* (NZEH) physiology under different CO_2 scenarios. Front. Microbiol. **4**: 155. doi:10.3389/fmicb.2013.00155

Sakshaug, E., and others. 1997. Parameters of photosynthesis: Definitions, theory and interpretation of results. J. Plankton Res. **19**: 1637–1670. doi:10.1093/plankt/20.3.603

Sarmiento, J. L., and others. 2004. Response of ocean ecosystems to climate warming. Global Biogeochem. Cycles **18**: 35. doi:10.1029/2003gb002134

Sciandra, A., J. Harlay, D. Lefèvre, R Lemée, P Rimmelin, M Denis, and J.-P. Gattuso, 2003. Response of coccolithophorid *Emiliania huxleyi* to elevated partial pressure of CO_2 under nitrogen limitation. Mar. Ecol. Prog. Ser. **261**: 111–122. doi:10.3354/meps261111

Sett, S., L. T. Bach, K. G. Schulz, S. Koch-Klavsen, M. Lebrato, and U. Riebesell. 2014. Temperature modulates coccolithophorid sensitivity of growth, photosynthesis and calcification to increasing seawater pCO_2. PLoS One **9**: e88308. doi:10.1371/journal.pone.0088308

Shi, D., Y. Xu, and F. M. M. Morel. 2009. Effects of the pH/pCO_2 control method on medium chemistry and phytoplankton growth. Biogeosciences **6**: 1199–1207. doi:10.5194/bg-6-1199-2009

Smith, H. E. K., and others. 2012. Predominance of heavily calcified coccolithophores at low $CaCO_3$ saturation during winter in the Bay of Biscay. Proc. Natl. Acad. Sci. USA **109**: 8845–8849. doi:10.1073/pnas.1117508109

Stojkovic, S., J. Beardall, and R. Matear. 2013. CO_2 concentrating mechanisms in three southern hemisphere strains of *Emiliania huxleyi*. J. Phycol. **49**: 670–679. doi:10.1111/jpy.12074

Suffrian, K., K. G. Schulz, M. A. Gutowska, U. Riebesell, and M. Bleich. 2011. Cellular pH measurements in *Emiliania huxleyi* reveal pronounced membrane proton permeability. New Phytol. **190**: 595–608. doi:10.1111/j.1469-8137.2010.03633.x

Taylor, A. R., A. Chrachri, G. Wheeler, H. Goddard, and C. Brownlee. 2011. A voltage-gated H^+ channel underlying pH homeostasis in calcifying coccolithophores. PLoS Biol. **9**: e1001085. doi:10.1371/journal.pbio.1001085

Thomas, M. K., C. T. Kremer, C. A. Klausmeier, and E. Litchman. 2012. A global pattern of thermal adaptation in marine phytoplankton. Science **338**: 1085–1088. doi:10.1126/science.1224836

Trimborn, S., G. Langer, and B. Rost. 2007. Effect of varying calcium concentrations and light intensities on calcification and photosynthesis in *Emiliania huxleyi*. Limnol. Oceanogr. **52**: 2285–2293. doi:10.4319/lo.2007.52.5.2285

Tyrrell, T., and A. H. Taylor. 1996. A modelling study of *Emiliania huxleyi* in the NE Atlantic. J. Mar. Syst. **9**: 83–112. doi:10.1016/0924-7963(96)00019-x

Utermöhl, H. 1958. Zur Vervollkommnung der quantitativen Phytoplankton-Methodik. Mitt. Internationale Ver. Theor. Angew. Limnol. **9**: 1–38.

Watabe, N., and K. M. Wilbur. 1966. Effects of temperature on growth calcification and coccolith form in *Coccolithus huxleyi* (coccolithineae). Limnol. Oceanogr. **11**: 567–575. doi:10.4319/lo.1966.11.4.0567

Webb, W. L., M. Newton, and D. Starr. 1974. Carbon dioxide exchange of alnus-rubra - a mathematical model. Oecologia **17**: 281–291. doi:10.1007/BF00345747

Welschmeyer, N. A. 1994. Fluorometric analysis of chlorophyll a in the presence of chlorophyll b and pheopigments. Limnol. Oceanogr. **39**: 1985–1992. doi:10.4319/lo.1994.39.8.1985

Westbroek, P., E. W. De Jong, P. Van der Wal, A. H. Borman, J. P. M. De Vrind, D. Kok, W. C. De Bruijn, and S. B. Parker. 1984. Mechanism of calcification in the marine alga *Emiliania huxleyi*. Philos. Trans. R. Soc. Lond. **304**: 435–444. doi:10.1098/rstb.1984.0037

Westbroek, P., E. W. De Jong, P. Van der Wal, A. H. Borman, J. P. M. De Vrind, D. Kok, W. C. De Bruijn, and S. B. Parker, 1993. A model system approach to biological climate forcing - the example of *Emiliania huxleyi*. Glob. Planet. Chang. **8**: 27–46. doi:10.1016/0921-8181(93)90061-r

Winter, A., R. W. Jordan, and P. H. Roth. 1994. Biogeography of living coccolithophores in ocean waters. Cambridge Univ. Press.

Woltereck, R. 1909. Weitere experimentelle Untersuchungen über Artveränderung, speziell über das Wesen quantitativer Artunterschiede bei Daphnien. Verh. Dtsch. Zool. Ges. **19**: 110–173. doi:10.1007/bf01876686

Young, J. R., and P. Westbroek. 1991. Genotypic variation in the coccolithophorid species *Emiliania huxleyi*. Mar. Micropaleontol. **18**: 5–23. doi:10.1016/0377-8398(91)90004-P

Young, J. R., M. Geisen, L. Cros, A. Kleijne, C. Sprengel, I. Probert, and J. Østergaard. 2003. A guide to extant coccolithophore taxonomy. J. Nannoplankton Res. Spec. Issue **1**: 1–125.

Ziveri, P., B. De Bernardi, K. H. Baumann, H. M. Stoll, and P. G. Mortyn. 2007. Sinking of coccolith carbonate and potential contribution to organic carbon ballasting in the deep ocean. Deep-Sea Res. II. **54**: 659–675. doi:10.1016/j.dsr2.2007.01.006

Zondervan, I. 2007. The effects of light, macronutrients, trace metals and CO_2 on the production of calcium carbonate and organic carbon in coccolithophores - a review. Deep-Sea Res. II. **54**: 521–537. doi:10.1016/j.dsr2.2006.12.004

Zondervan, I., R. E. Zeebe, B. Rost, and U. Riebesell. 2001. Decreasing marine biogenic calcification: A negative feedback on rising atmospheric pCO_2. Global Biogeochem. Cycles **15**: 507–516. doi:10.1029/2000gb001321

Zondervan, I., B. Rost, and U. Riebesell. 2002. Effect of CO_2 concentration on the PIC/POC ratio in the coccolithophore *Emiliania huxleyi* grown under light-limiting conditions and different daylengths J. Exp. Mar. Biol. Ecol. **272**: 55–70. doi:10.1016/s0022-0981(02)00037-0

Conflict of Interest

None declared.